UCLouvain

École polytechnique de Louvain

Simulating pathological gait using Geyer's neuromuscular model

Author: **Simon Messens**
Supervisor: **Renaud Ronsse**
Readers: **Paul Fisette, Henri Laloyaux**
Academic year 2023–2024
Master [120] in Biomedical Engineering

Abstract

The ability to walk is essential for both physical and mental health. Disruptive gait disorders can significantly impact a patient's quality of life. The development of technologies to alleviate these effects is crucial and the field of research is both mature and rapidly evolving. Solutions such as passive and active prostheses or exoskeletons can positively enhance the patient's locomotion, but testing new designs can pose a significant risk if the device-patient interaction produces unexpected behavior leading to falls or injuries.

To mitigate this risk, this thesis aims to propose a simulation for pathological gait, creating a safe environment to test and develop new walking assistive aids.This approach is based on Geyer's neuromusculoskeletal reflex model, which was partially translated from its Simulink implementation to Python by M. Aussems and N. Dineur in their 2023 thesis. This implementation was completed and refined and a reflex adaptation method was developed to tune the biped controller to new musculoskeletal conditions while achieving predetermined metrics.

Testing the adaptation on a healthy gait yielded a bipedal model that matched the expected biomechanics of a specific gait, with further analysis on the inner kinetics and kinematics. This method was then applied to model the effects of aging on muscle, testing its ability to predict patient behavior under specific constraints and extract its characteristics to compare to known trends, yielding mixed results.

The results of this thesis take steps towards in silico prediction of patient responses to pathology and assistive inputs, thereby reducing the risk of unwanted and dangerous behaviors.

Acknowledgement

First, I would like to express my deepest gratitude to my supervisor, Prof. Renaud Ronsse, for his guidance and invaluable insights throughout the year.
Second, I cannot thank Henri Laloyaux enough for our weekly meetings, which kept me on track through the ups and downs and always provided solutions and optimism.
I also want to thank my family for their unwavering support throughout this master thesis and my entire engineering journey; your support and encouragement have meant more to me than you know.
A special thanks to Maeva Aydin for her patience and willingness to discuss bipedal locomotion and optimization more times than she probably should have.
Lastly, thanks to Benoît Jacques.

Contents

Chapter 1

Foundations

1.1 Introduction

Walking, a fundamental human function, is crucial not only for mobility but also for overall quality of life [1]. It facilitates environmental interactions, supports daily activities and is essential for both physical and mental well-being. Gait metrics have been shown to predict aspects of an individual's well-being and life expectancy [2, 3].

However, individuals suffering from gait pathology experience considerable difficulties in walking. These pathologies can stem from various sources such as neurological disorders [4], musculoskeletal abnormalities, injuries, or the natural aging process [5]. Manifestations of these conditions include unsteady or altered gait, challenges in initiating movement, imbalance, or diminished walking speed. These impairments significantly affect an individual's independence and their ability to engage fully in societal roles.

The demographic shift towards an older population is becoming one of the main challenges for industrialized nations. Projections indicate that in 40 years, over 20% of Europe's population will be older than 60 years [6]. This aging demographic underscores the urgent need for innovative therapeutic technologies. Prosthetics, orthotics and exoskeletons offer promising avenues to either restore or augment locomotive abilities. The success of these technologies, however, critically depends on the precision of control strategies that must predict and precisely react to the user's natural gait patterns and responses.

Developing assistive devices is complex and testing them is potentially dangerous for patients. Having reliable models to predict patient reactions can significantly reduce risks and the effort needed for development. Each disease may introduce anomalies in muscle activation, leading to differences in the gait cycle. The ultimate goal is to predict patient behavior more precisely when anomalies are introduced,

thereby proposing more effective assistive solutions.

This thesis builds upon the foundational work of Hartmut Geyer [7], who developed a simplified yet effective neuromuscular model based on muscle reflexes. Previously, Geyer's model has been implemented in MATLAB/Simulink, which requires additional costly licenses, limiting its accessibility. The goal of this thesis is to adapt and implement Geyer's model for pathological gait within a Python framework, using open-source tools such as Robotran to ensure wider availability and facilitate advancements in gait analysis and assistive device development.

Building upon the foundational work by Matthieu Aussems and Nicolas Dineur [**?**], who initiated the adaptation of Geyer's model to a Python environment, this thesis has significantly expanded the scope and depth of the model's application. The previous work successfully created a comprehensive bipedal model, but lacked the ability to simulate a walking gait. This thesis has successfully addressed these challenges, enhancing the model's performance and extending its applicability to include a broader range of pathological conditions and aging effects.

The thesis is structured into several key phases: initially, a deep theoretical exploration of Geyer's model and its applications to pathological gait; followed by the practical implementation of the model in python; an optimization method was developed to adapt the reflex to new neuromusculoskeletal conditions; and finally, a thorough validation of the model through comparative analysis with existing implementations and comparative studies of pathological gait.

All tools, models and simulations developed during this thesis will be openly shared to foster further research and development in the field.

All tables, graphs, and code included in this thesis are accessible on Github [8]. Additionally, text correction and reformulation were supported by the AI tool ChatGPT, in line with EPL's guidelines.

1.2 The Human Gait

To understand the human gait, we first need to understand the 3D coordinates of the body. The standing position of the bipedal model is used to define the three anatomical planes. Conventionally, the z-axis points upwards, the y-axis points to the left side of the model and the x-axis points forwards.

- The frontal plane, also known as the coronal plane, is oriented vertically and divides the body into front (anterior) and back (posterior) sections. It is aligned with the yz-plane.
- The sagittal plane is another vertical plane that splits the body into right and left halves. It runs parallel to the xz-plane.

- The transverse plane, sometimes referred to as the horizontal plane, is perpendicular to both the frontal and sagittal planes. It separates the body into upper (superior) and lower (inferior) portions and lies parallel to the yx-plane.

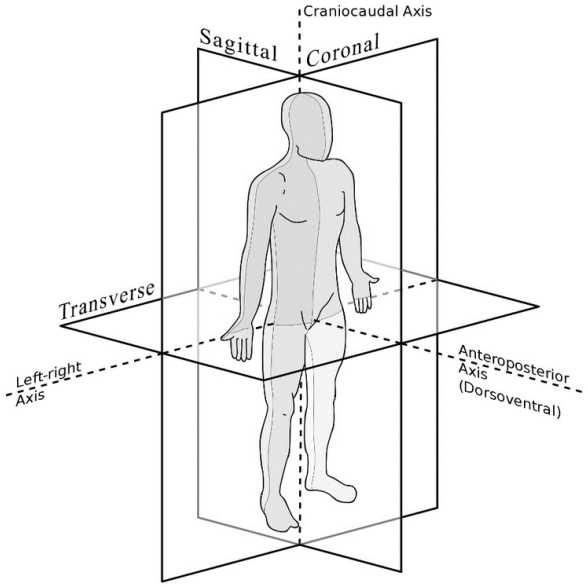

Figure 1.1: Representation of the 3D planes from [9].

1.2.1 Gait Cycle

The gait cycle of a leg consists of two primary phases: the stance phase and the swing phase. According to Kharb [10], the stance phase is the period during which the leg is in contact with the ground, supporting the weight of the body. Conversely, the swing phase is when the leg moves forward through the air.

In a complete gait cycle, each leg undergoes one full cycle. In a typical healthy gait, the leg spends approximately 60% of the cycle in the stance phase and 40% in the swing phase [10]. Pathological conditions can lead to deviations from this pattern [11]. Additionally, for about 20% of the gait cycle, both feet are in contact with the ground, known as the double support phase.

Starting with the right heel making contact with the ground, the walking cycle can be divided into four distinct phases:

1. **Double Support Phase I:** Both feet touch the ground.

2. **Single Support Phase I:** The left leg enters the swing phase after the left toes lift off the ground, with the right leg remaining in the stance phase.

3. **Double Support Phase II:** The left heel contacts the ground, resulting in both feet being in contact with the ground.

4. **Single Support Phase II:** The right leg enters the swing phase after the right toes lift off the ground, the left leg remains in the stance phase.

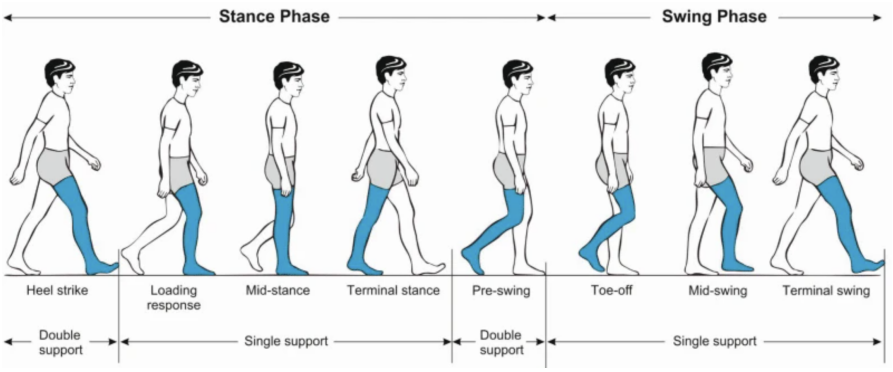

Figure 1.2: Representation of the gait cycle [12].

1.2.2 The Components

Gait is a coordinated activity involving various anatomical and physiological components:

Joints

The hip, knee and ankle joints facilitate major movements. The hip provides stability and propulsion, the knee allows for shock absorption and leg extension and the ankle aids in foot clearance and push-off.

Muscles

Key muscles include the quadriceps, hamstrings, gluteal muscles, calf muscles and tibialis anterior. Proper timing and intensity of muscle contractions are essential for smooth and efficient gait.

Bones

The femur, tibia, fibula and foot bones form the structural framework supporting body weight and facilitating movement. The pelvis connects the spine to the lower limbs, playing a critical role in balance and weight transfer.

Brain and Nervous System

The central nervous system (brain and spinal cord) coordinates voluntary movements and processes sensory feedback. Reflexes, such as the stretch reflex, help maintain posture and adapt to changes in terrain.

Ground Interactions

Ground reaction forces are crucial for propulsion and balance. Proper foot mechanics ensure effective force distribution and shock absorption.

Proprioception and Sensory Feedback

Proprioception involves sensory receptors in muscles and joints providing information about body position and movement. Sensory feedback from visual, vestibular and somatosensory inputs helps maintain balance and adjust movements in real-time.

Understanding these components is vital for analyzing both normal and pathological gait, enabling the development of targeted interventions and treatments.

1.3 Simulating/Modeling Human Gait

Human gait analysis is a complex problem in biomechanics due to the highly nonlinear nature of human motion equations, muscle dynamics and foot-ground contact. Despite numerous studies in this field, predictive human gait simulation remains a significant challenge [13]. Various models have been developed by researchers aiming to enhance accuracy and computational efficiency for various evaluative studies, such as model-based assistive device controllers, surgical intervention planning, athletic training and prosthesis and orthosis design [14].

Human models used in gait simulation can be broadly classified into skeletal (SK), musculoskeletal (MSK) and neuromusculoskeletal (NMSK) models [15].

- **Skeletal Models**: These are the simplest form of human models used in gait analysis. They primarily focus on the rigid body dynamics of the skeleton, excluding muscle activation dynamics, muscle contraction dynamics and musculoskeletal geometry. Skeletal models are useful for understanding the

basic kinematics and kinetics of human movement but lack the detail required to simulate muscle forces and activations accurately.

- **Musculoskeletal Models**: Building upon skeletal models, musculoskeletal models add a layer of complexity by including muscle contraction dynamics and musculoskeletal geometry. These models simulate how muscles generate forces and how these forces are transmitted through the skeletal system to produce movement. However, they do not account for muscle activation dynamics, which limits their ability to simulate the neural control of movement.
- **Neuromusculoskeletal Models**: These are the most comprehensive and complex models used in gait analysis. Neuromusculoskeletal models incorporate all aspects of muscle activation dynamics, muscle contraction dynamics and musculoskeletal geometry. They simulate the entire process of movement generation, from neural activation to muscle contraction to skeletal movement. This makes them highly valuable for studying the interactions between the nervous system, muscles and skeleton in producing movement, as well as for developing and testing assistive devices and therapeutic interventions.

1.3.1 Neuromusculoskeletal Bipedal Models

The neuromusculoskeletal bipedal model used in this thesis is a comprehensive mathematical representation of the human body, integrating the skeletal, muscular and nervous systems along with their interactions with the external environment. This model is pivotal for simulating human gait and understanding the underlying biomechanics.

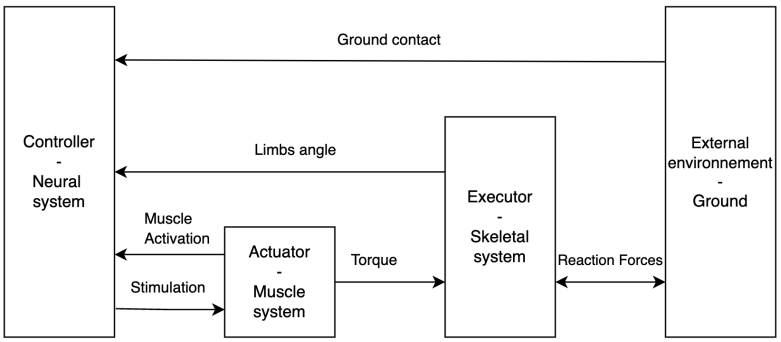

Figure 1.3: Neuromuscular control system interaction diagram.

Model Components and Control Mechanisms

As shown in Fig 1.3, the biped comprises three main subsystems, each with specific control and feedback mechanisms, with an additional system being the external environment:

- **Skeletal System:** This system includes a trunk segment and three-segmented legs, representing the rigid body dynamics of the human skeleton. The skeletal system acts as the executor, moving the limbs according to the actuator's commands and the forces encountered from the ground and the surrounding environment.
- **Muscular System:** The muscular system is modeled using Hill-type muscles, which simulate muscle contraction dynamics. In the sagittal plane, seven Hill-type muscles are used, with an extension to a 3D model that includes additional muscles for coronal plane movements. The actuator processes instructions from the controller to activate these muscles.
- **Nervous System:** The nervous system is represented through sensory reflexes, controlled by feedback mechanisms responsive to force and length. This subsystem is crucial for simulating the neural control of movement. The controller sends instructions to the actuator based on feedback from other components.
- **External Environment:** The ground exerts a force on the contact points of the feet, which acts on the skeletal system and provides sensory information to the nervous system.

Modeling Limitations

In developing the neuromusculoskeletal bipedal model, assumptions and choices where made to simplify the complex interactions within the human body and to make the simulation computationally feasible:

- **Dimensionality Reduction:** The model operates primarily in a 2D environment to reduce the computational complexity, focusing on the sagittal plane which is most relevant for basic gait analysis.
- **Muscle Simplification:** The number of muscles is reduced in the model. Only key muscles involved in major gait functions are included, which simplifies the muscle dynamics without significantly compromising the accuracy of the simulation [15].

- **Reflex Mechanisms:** Reflexes are modeled as simple feedback loops without higher-level cognitive processing. This limitation allows for the simulation of basic motor control without the need for complex neural network models.
- **No Reaction to External Stimuli:** The model does not account for visual or auditory feedback, focusing solely on proprioceptive and force feedback mechanisms. This simplifies the control system but limits the model's ability to simulate reactions to external disturbances.
- **Ground Contact Model:** Physics modeling is always an approximation of real life and this is particularly evident in ground contact and stiff body problems. The ground reaction forces (GRF) are modeled using simplified contact mechanics, which provide a reasonable approximation for gait analysis but may not capture all the complexities of foot-ground interactions.

These limitations are necessary to make the model computationally tractable while still providing valuable insights into the biomechanics of human gait. They represent a balance between complexity and feasibility, ensuring that the model remains useful for both research and practical applications in gait analysis and assistive device development.

1.3.2 Geyer's Model

Hartmut Geyer and Hugh Herr developed a neuromuscular model [16] that significantly contributes to our understanding of human locomotion by integrating principles of legged mechanics with muscle reflexes. Their model, detailed in the paper "A Muscle-Reflex Model That Encodes Principles of Legged Mechanics Produces Human Walking Dynamics and Muscle Activities" [17], which has been cited 473 times, emphasizes the role of muscle reflexes in stabilizing and adapting human gait under various conditions without the need for extensive central control interventions.

The model is shown in Fig 1.4 represents the human body with a trunk and two three-segment legs, each leg being actuated by seven Hill-type muscles with three pairs of joints. This setup allows for a direct comparison with prominent muscles of the human leg, providing insights into human walking dynamics, leg kinematics and muscle activation patterns.

Muscle Mechanics in Geyer's Model

Geyer's model employs a sophisticated representation of muscle dynamics using the Hill-type muscle model, which is crucial for simulating realistic human gait.

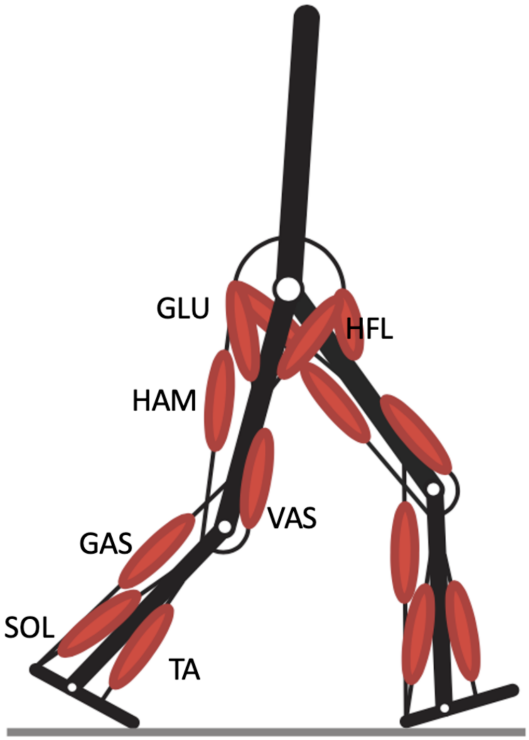

Figure 1.4: The seven pairs of muscles of the bipedal model.

This model incorporates both the active and passive properties of muscle tissues, making it highly effective for studying neuromuscular control and biomechanics.

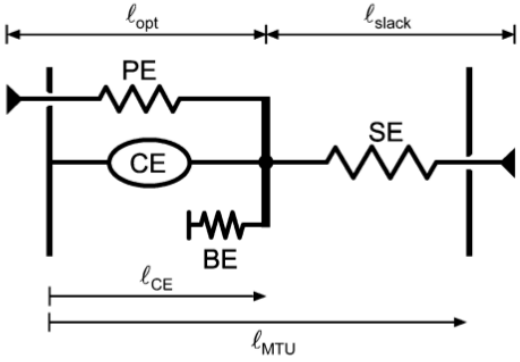

Figure 1.5: This diagram available in Geyer paper [17] describe the muscle-tendon model. The diagram shows the interaction between the contractile element (CE), series elasticity (SE), parallel elasticity (PE) and buffer elasticity (BE), forming the complete Muscle-Tendon Unit (MTU).

This detailed muscle modeling allows the neuromuscular model to simulate human walking dynamics with high fidelity.

- **Active Contractile Element (CE):** The CE is responsible for generating force based on nervous activation and muscle fiber length. It simulates the force-length and force-velocity properties of muscle fibers, which are fundamental to muscle function.
- **Series Elasticity (SE):** The SE represents the tissue connected to the muscle fibers. It stores and releases elastic energy during muscle contractions and extensions, which is essential for efficient movement.
- **Parallel Elasticity (PE):** The PE component models the non-contractile elements in the muscle that contribute to passive force when the muscle is stretched beyond its resting length. This helps in protecting the muscle from excessive stretching.
- **Buffer Elasticity (BE):** This component prevents the collapse of the active contractile element when the series elasticity is slack, ensuring that the muscle can still generate force under various lengths.

These components are integrated into a Muscle-Tendon Unit (MTU), which interacts dynamically with the skeletal system through joint torques. The MTU's behavior is governed by the following equation, which balances the forces between the CE, SE, PE and BE:

$$F_{total} = F_{CE}(activation, length, velocity) + F_{SE}(length) + F_{PE}(length) - F_{BE}(length)$$

This equation ensures that the muscle's response is biomechanically realistic.

1.3.3 Muscle Activation

To attain a higher level of realism, the muscle activation (A_m) is derived from muscle stimulation (S_m). This process introduces a time delay, which can be modeled using a first-order differential equation:

$$\tau \cdot \frac{dA_m(t)}{dt} = S_m(t) - A_m(t)$$

This equation acts as a low-pass filter with a time constant τ of 0.01 seconds, smoothing the rapid changes in muscle stimulation to produce a more gradual muscle activation response. The dynamic response of muscle activation is illustrated in the Figure 1.6.

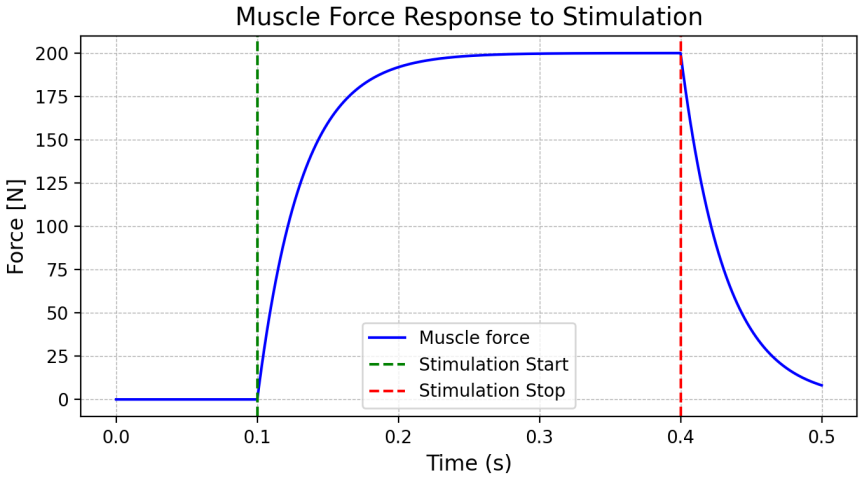

Figure 1.6: Dynamic response of muscle activation

The time constant τ is crucial as it determines the rate at which muscle activation responds to changes in stimulation. A smaller τ would result in a faster response, while a larger τ would slow down the activation process. This modeling approach helps in accurately simulating the physiological delay between neural stimulation and muscle contraction, which is essential for realistic gait simulation.

1.3.4 Reflex and Fixed Parameters

In the development and optimization of neuromuscular models like Geyer's, it is crucial to distinguish between fixed parameters and reflex parameters. Fixed parameters are typically derived from empirical data and represent physiological constants that do not change under normal conditions. Reflex parameters, on the other hand, can vary from one individual to another and may also be adjusted to simulate different conditions or pathologies. Broadly speaking the fixed parameters are the actuator and executor while the reflex parameters are the controller.

Fixed Parameters

Fixed parameters in the model include aspects such as muscle fiber compositions, anatomical constraints or the maximum muscle force possibly exerced by a muscle (F_{max}). These parameters are usually determined through rigorous experimental studies and are essential for ensuring that the model behaves in a physiologically realistic manner.

For example, F_{max} for each muscle is derived from biomechanical experiments that measure the maximum isometric force that muscle fibers can exert. These

values are crucial for the model as they define the upper limits of force production capability for the simulated muscles.

- **Maximum Muscle Force (F_{max}):** This parameter represents the peak isometric force that a muscle can generate.
- **Optimal Muscle Fiber Length (l_{opt}):** This is the muscle fiber length at which the muscle can generate its maximum force.
- **Maximum Contraction Velocity (v_{max}):** This parameter indicates the maximum speed at which a muscle can shorten. It is crucial for modeling dynamic muscle behavior and is usually obtained from experimental data.
- **Tendon Slack Length (l_{off}):** This is the length of the tendon when the muscle is at its optimal length and not generating any force. It is important for accurately modeling the muscle-tendon dynamics.
- **Joint Constraints:** Joint ranges of motion are dependent on the biomechanical constraint of the human body.

In the case of Geyer's model, these values were estimated from various sources [18–20] and adapted to the specific problem at hand. While these will not be changed for a healthy gait, they could be adapted to simulate a pathological gait.

Reflex Parameters

Reflex parameters are adjustable within the model to simulate how different neural control strategies can affect movement. These include thresholds for muscle activation, reflex gains and adaptation speeds. Adjusting these parameters can help simulate how individuals with different neuromuscular conditions might experience and compensate for their impairments.

- **Reflex Gains:** These parameters control the intensity of the response from sensory feedback. Higher gains can lead to more robust responses but can also result in instability if not properly tuned.
- **Threshold for Muscle Activation (θ_{ref}):** This parameter determines at what point a muscle begins to activate in response to a stretch or load.
- **Desired Joint Angles:** These parameters set the target angles for specific joints during movement. Adjusting these angles can help simulate different gait patterns and postural adjustments, which is particularly useful for studying pathological conditions or optimizing rehabilitation strategies.

Geyer determined the optimal values for these reflex parameters through an optimization process aimed at achieving specific gait metrics, such as a walking speed of 1.3 m/s. This optimization involved adjusting the parameters to minimize the metabolic cost of walking while maintaining stability and realistic movement patterns. The Figure 1.7, extracted from Geyer's work [17], lists the reflex parameters and their respective ranges.

TABLE I

REFLEX PARAMETERS AND THEIR TOLERANCE. GAINS G_m AND k_{bw} ARE NORMALIZED TO $F_{\mathrm{max,m}}$ AND THE BODY WEIGHT. OFFSETS $\ell_{\mathrm{off,m}}$ ARE SHOWN IN FRACTIONS OF $\ell_{\mathrm{opt,m}}$. PRESTIMULATIONS $S_{0,m}$ ARE 0.01 (NOT SHOWN) EXCEPT FOR THE STANCE VALUES $S_{0,\mathrm{VAS}}$ AND $S_{0,\mathrm{BAL}}$ OF THE VAS AND OF THE TRUNK BALANCE MUSCLES HAM, GLU AND HFL

	value	min ... max		value	min ... max
G_{SOL}	1.2	0.97 ... 2.17	θ_{ref}	0.105	0.017 ... 0.11
G_{TA}	1.1	0.55 ... 3.2	k_d	0.25	0.10 ... 0.75
$\ell_{off,TA}$	0.71	0.59 ... 0.80	k_{bw}	1.2	1.3 ... 5.0
G_{SOLTA}	0.3	0 ... ∞	ΔS	0.25	0.14 ... 1
G_{GAS}	1.1	0 ... ∞	G_{HAM}	0.65	0 ... 0.67
$S_{0,VAS}$	0.09	0.047 ... 0.71	G_{GLU}	0.4	0 ... 0.52
G_{VAS}	1.15	0.82 ... 13.5	G_{HFL}	0.35	0.17 ... 3
k_φ	2	0 ... ∞	$\ell_{off,HFL}$	0.6	0 ... 0.67
$\varphi_{k,off}$	2.97	2.71 ... ∞	G_{HAMHFL}	4	0 ... 100
$S_{0,BAL}$	0.05	0.01 ... 0.32	$\ell_{off,HAM}$	0.85	0.83 ... ∞
k_p	1.91	1.78 ... 22	k_{lean}	1.15	1 ... 5.7

Figure 1.7: Table of Reflex Parameters extracted from Geyer's paper

The table includes parameters such as muscle-based gains (G_m), length offsets (l_{off}) and various other reflex-related constants. These parameters were fine-tuned using an optimization function that iteratively adjusted them to achieve the desired walking speed and stability. The optimization process considered the complex interactions between the neuromuscular and skeletal systems, ensuring that the resulting gait was both efficient and biomechanically realistic.

Chapter 2

Implementation

2.1 Architecture

2.1.1 Simulink

Simulink is a graphical programming environment for modeling, simulating and analyzing dynamic systems. It uses pre-built blocks to represent signals, mathematical functions, filters and more, making it particularly well-suited for signal processing and control modeling. Simulink is a MATLAB-based graphical programming environment for modeling, simulating and analyzing multidomain dynamical systems. Its primary interface is a graphical block diagramming tool and a customizable set of block libraries.

Furthermore, Simulink offers various add-on modules, such as Simscape, which is the physical modeling component within the Simulink environment. Simscape facilitates the construction of multibody systems.

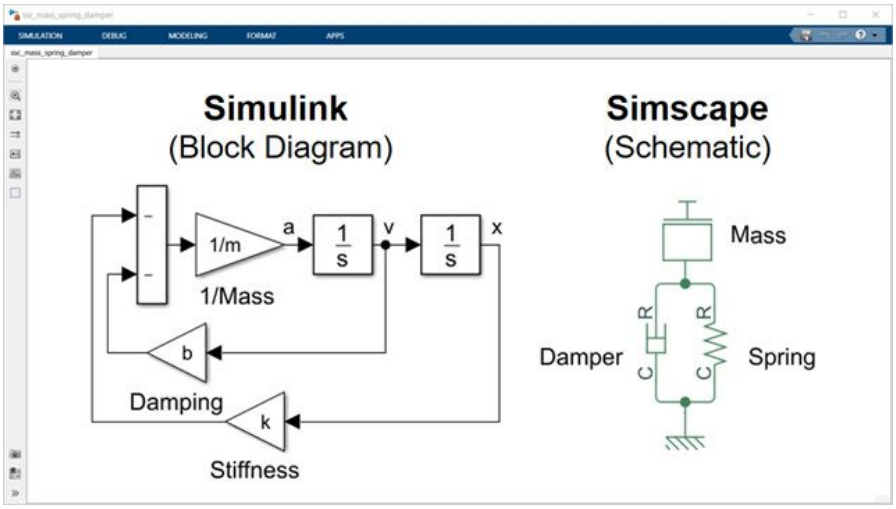

Figure 2.1: Simulink model with Simscape integration [21]

The original implementation of Geyer's model was done in Simulink [22].

2.1.2 Python - Environment

The Python implementation utilizes the Robotran [23] environment, developed at UCL-MEED. Robotran is a robust tool designed for generating dynamic and kinematic equations of multibody systems (MBS) using a symbolic approach. The system's graphical description in MBsysPad allows for the generation of multibody equations in Python through the symbolic translator MBsysTran. These equations can subsequently be accessed via the MBsysSIM interface and a 3D animation can be executed using the 3D illustrator.

As per the Figure 2.2, the stack uses a multibody system. It is a sophisticated mechanical assembly consisting of multiple interconnected bodies that interact through joints. The dynamics and motion of each body within the system are governed by the forces and torques applied by other bodies and external influences. The multibody system relevant to this thesis is depicted in the Figure 2.3.

Each leg in the system features three revolute joints with rotation axes perpendicular to the sagittal plane. These legs are connected to the trunk via an additional sagittal revolute joint. The thigh segment is divided into two parts (upper and lower thigh) connected by a prismatic transversal joint. This segmentation is crucial for determining the mass distribution across the body's two legs, which is essential for calculating muscle stimulations.

The model is anchored to the inertial frame (Base) using three prismatic and three rotational joints, providing six degrees of freedom. However, in a 2D model, only four joints are necessary. Each foot is equipped with two sensors: one at the

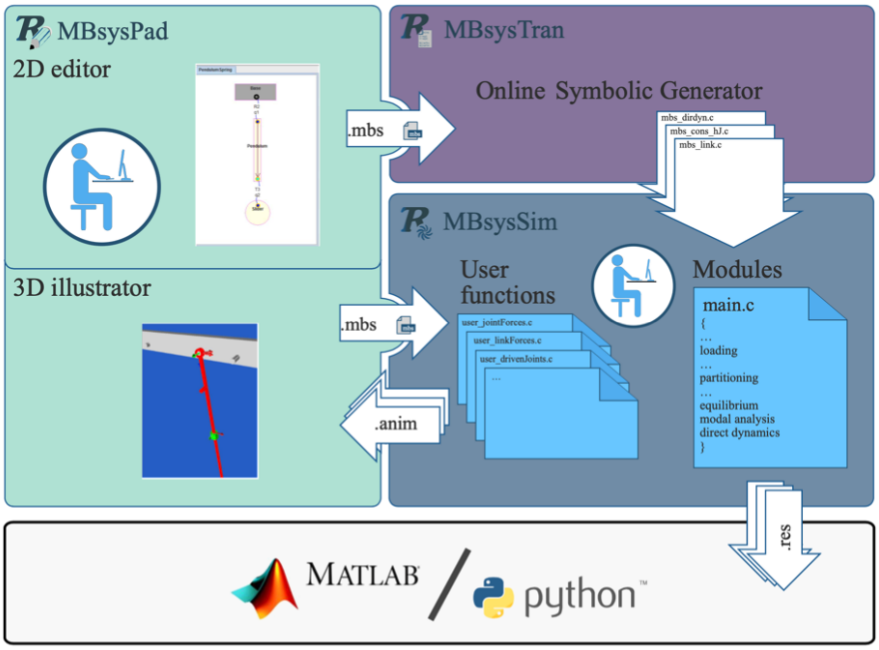

Figure 2.2: Robotran environment for generating dynamic and kinematic equations of multibody systems

heel and another at the toe. These sensors continuously monitor the feet positions, enabling real-time calculation of external forces. Additionally, two sensors are placed on the trunk to measure its pitch angle.

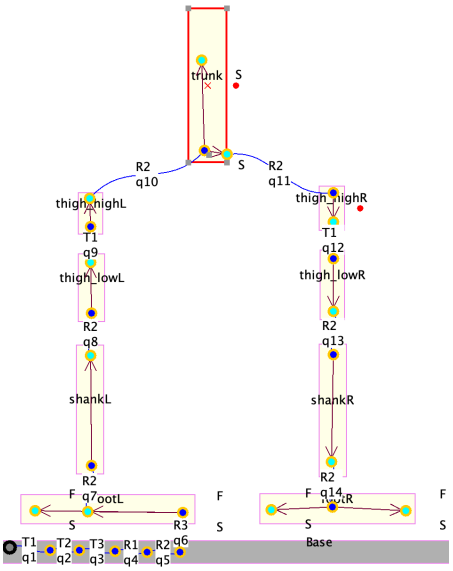

Figure 2.3: Robotran representation of the multibody system representing the lower limbs and trunk of a human via MBsysPad. [23]

2.1.3 Aussems - Dineur version

While the theoretical basis is Geyer's model, the implementation of the python model is based on the Aussems - Dineur version. Their work was the basis of the current analysis [24].Aussems and Dineur's thesis aimed to replicate and implement Geyer's walking model using the combination of python and Robotran, making it accessible in a widely used programming language with open source software. Their work followed a three-stage approach: theoretical understanding, practical implementation and validation against Geyer's Simulink model.

While the quantity and quality of their work was undeniable, their model did not attain the expected results. They implemented each modules and dependencies needed for the development of a bipedal model but did not have the time to properly test them as a whole. As a result discrepancies went unnoticed and influenced its behavior eventually causing a fatal collapse after 1.8s of simulation-time as can be seen on the Figure 2.4.

More precisely after the 1.42s mark, a noticeable issue appeared during the swing phase of the right leg. The right foot entered in contact with the ground prematurely and it's unexpected position caused an unbalance. This phenomenon was responsible for the collapse but its inner causes where not fully identified by the previous team.

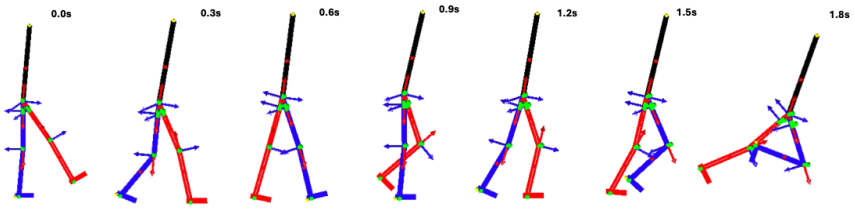

Figure 2.4: Gait cycle animation from Aussems and Dineur's model.

2.1.4 Work to Update the Aussems - Dineur version

A significant part of this thesis was dedicated to updating the Aussems - Dineur version. Below is a summary of the main issues identified and the corresponding updates made:

Model Accuracy and Stability

- **Ground Contact Model:** The Ground Reaction Force (GRF) was not correctly programmed to follow Simulink, causing fatal crashes. This was fixed to prevent resonance issues when the foot strikes the ground at a flat angle.
- **Interpolation error:** The current length of the muscle, lce_curr, calculation is done using interpolated valued based on past length but incorrectly set up so it predicted the current length as the length of two iteration ago.
- **Neural Control Layer:** Indices for past muscle activation (5ms, 10ms, 20ms) were miscalculated, causing improper muscle activation. This was fixed.
- **Dimension Errors:** Previously incorrect dimensions for the msbpad biped (size and weight distribution of feet) were corrected.
- **Sensor Allocation:** Some sensors were pointing to the wrong body parts, causing unexpected model behavior. This was adjusted.
- **Muscle Activation:** Incorrect settings for the maximum isometric force of a muscle F_max_muscle led to improper muscle activation. This was corrected.
- **Inter-execution variable reload:** In some context the robotran module was not reloaded between execution leading to variable being kept in memory longer than expected and not reseted.

System Compatibility and Execution

- **Computer Agnosticism:** The model was initially tailored to specific machines (Mathieu Aussems' machine and MacOS). It was updated to run on any computer with any OS.
- **Execution Framework:** Improper comprehension of the Robotran framework in executing individual files led to incorrect torque calculations. The *joint_force.py* file is responsible for calculating the torques for the joints. Robotran processes this script one time for each currently observed body/limb. In our case, this means three times at each step of the simulation, with exceptions leading to two executions per timestep. This misunderstanding resulted in torques being twice or thrice greater than expected. To correct this, some delta time in integration steps were blindly adapted to match the expected results, leading to a time-consuming process to verify and change most of them.
- **Delta Time Transmission:** Delta time was not properly transmitted, leading to imprecise calculations. This was fixed.
- **Fixed Time Steps:** Time steps were hard-coded in two separate places with different values, leading to inconsistencies. This was fixed to ensure coherence.

Performance Optimization

- **Memory Management:** The previous model stored past memory indefinitely, leading to excessive memory usage (960MB per simulation second). This was optimized to store only the last 20ms of data, reducing execution time by over 96% (from 90 minutes to 3.6 minutes for 1.5s simulation). The current benchmark is 1.5 minutes for 1.5s execution.

2.1.5 First steady state Python version

Significant effort led to the development of the first steady-state version. It is now capable of simulating a plausible walking gait indefinitely without falling or any detectable anomalies. The variation between gait cycles is also minimal.

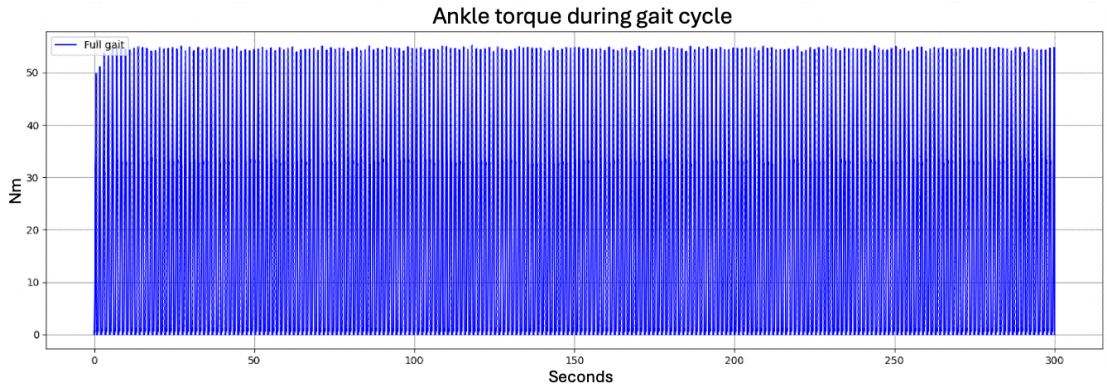

Figure 2.5: Full Ankle Torque Profile

The Figure 2.5 shows the variation of torques in the ankle of a simulated biped during a 300-second simulation. The cyclical nature of a walking gait is visible with spikes appearing at regular intervals, indicating a steady state in the walker.

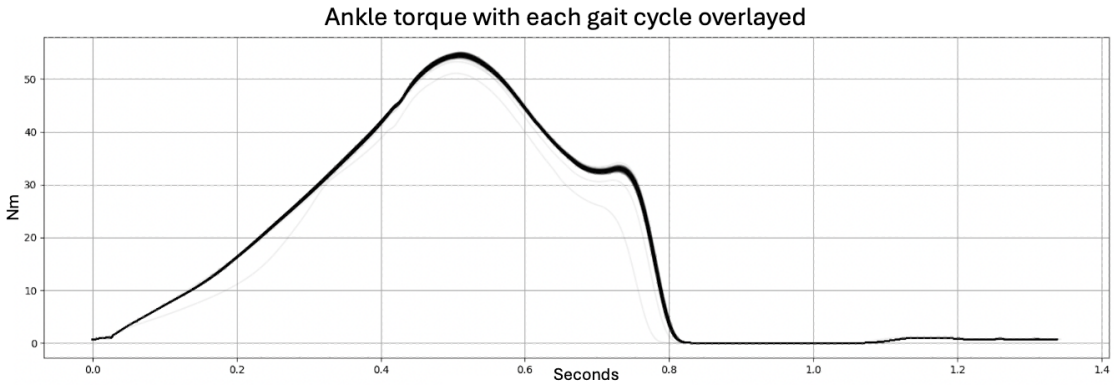

Figure 2.6: Overlayed Ankle Torque Comparison

The Figure 2.6 shows the intra-cycle variability by overlaying the ankle torque for each cycle. It was created by plotting the torque for each individual cycle on top of one another using a fine grey line. The start of the cycle was determined by the moment the toe touches the ground. This exposes the intra-cycle variability, with a visible black region showing that torques are similar between cycles, with two thin lines outside the normal range corresponding to the start of the model.

Comparison to the Simulink model

This model was built using the implementation method and parameters of the Simulink model to be as close to a carbon copy of it as possible. However, while

the gait cycle seems anatomically correct, its biomechanical metrics did not match those of the Simulink implementation.

To ensure accuracy and reliability for future research, it is crucial to match the Simulink model's biomechanical metrics. This alignment serves as a validated benchmark, validating the Python model's effectiveness and suitability for ongoing research and development.

The most glaring discrepancy is the speed of both models. Geyer described a 1.3 m/s target for his model, which was achieved in the Simulink version, while this Python version averaged 0.97 m/s.

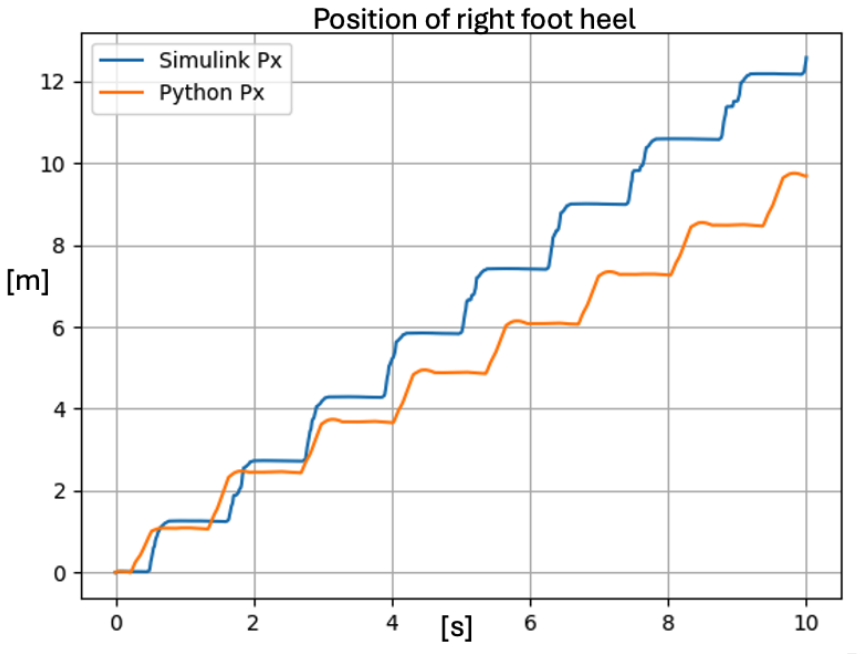

Figure 2.7: Comparison of the position of the foot for both models

The Figure 2.7 shows the position of the right foot for both models. The overall speed does not match and the finer details diverge as well. The Python model tends to start its first swing phase for the right foot earlier, while the Simulink model has wider swings. These divergences between the two models are problematic when using Geyer's work as a basis to build upon.

2.1.6 Causes of Divergence

A neuromuscular bipedal model is inherently complex and interdependent. Changes in one part can impact the entire model. The impact of different choices and solver particularities is hard to quantify with certainty.

First, the solver used by Simulink/Matlab is ode15s [25], a variable-step, variable-order solver that has no direct equivalent in Robotran. Additionally, the previous team chose to use fixed timesteps which was continued in this work. This choice was made to facilitate numerous calculations since the biped model requires the value of past muscle activation in the reflex and stimulation calculations. These calculations were easily managed in the Simulink environment since it is based on a block diagram system, adding a layer of abstraction to the timesteps.

The goal of moving from Simulink to Python is to allow for more flexibility. Having fixed steps hinders the accuracy of the ground contact model but meets this goals and facilitate the implementation of diseases and other biological changes in the model.

1. **Time Step Variability**: The Simulink model's continuous mode with variable time steps was not replicated in the Python model. Implementing this requires identifying the parameters that dictate the time steps, which depend on both the software and the model states.

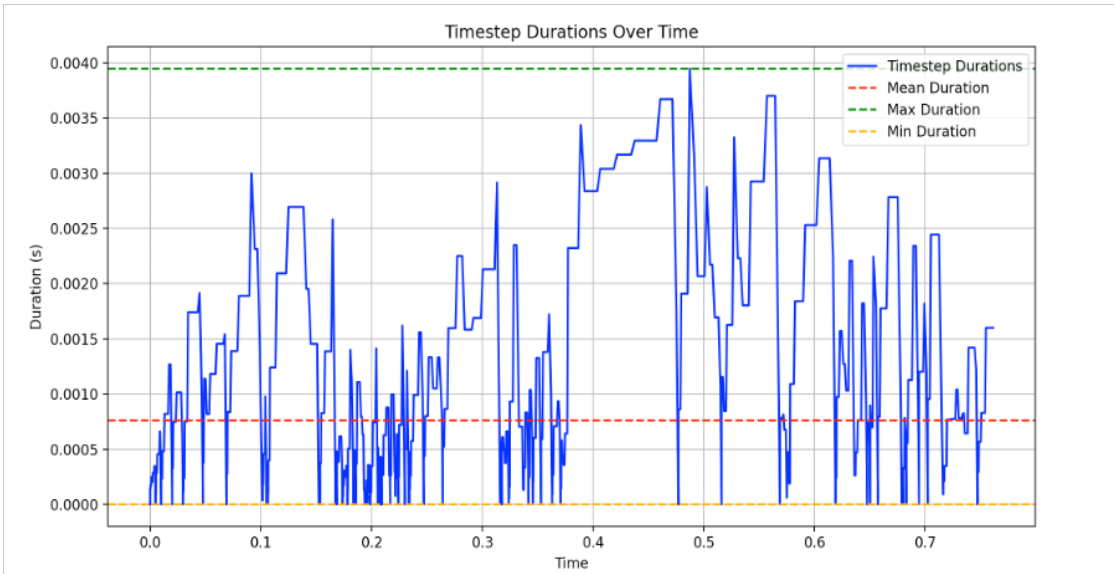

Figure 2.8: Variability in Time Steps

As shown in the Figure 2.8, Simulink time steps vary with an average of 0.75ms. For reproducibility and maintenance, the Python model uses a fixed 1ms time step.

2. **Ground Contact**: The ground contact modeling differs between the two models. To illustrate this, a test was conducted in an unactuated mode where

all forces on the joint were disabled. This test allows to observe how the Ground Reaction Force (GRF) of both models reacted under supposed similar conditions. Visually, the collapses of the skeletal (unactuated) model appear similar in both cases, but a more detailed analysis reveals subtle differences in how the foot remains or slips on the ground.

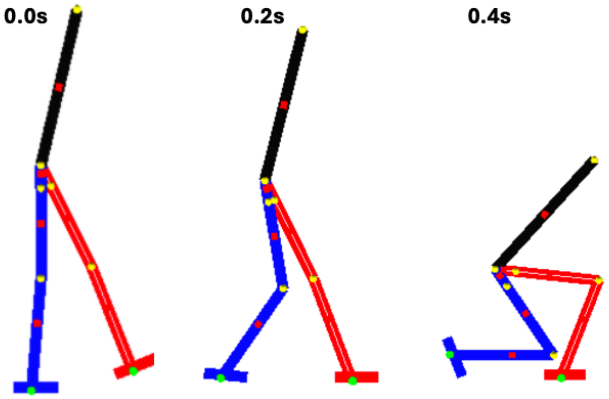

Figure 2.9: Representation of the unactuated test for the python model

The Figure 2.9 reveals the starting condition of the test, note that the right leg is shown in red.

The Figure 2.10 depict the evolution position of the right foot in the horizontal direction for both model and their delta. As can be seen the differences begin from the start, this is caused by the left foot of the python model slipping about 1.5cm backward at the start. This small starting difference will be compounded once the right feet touches the ground at 0.17s where the python model will slip further. Interestingly both feet position seems to converge at 0.4s under the constraints of the skeletal model collapsing in the same way. This once again demonstrate that small difference can lead to similar looking behavior but with marked kinematic differences.

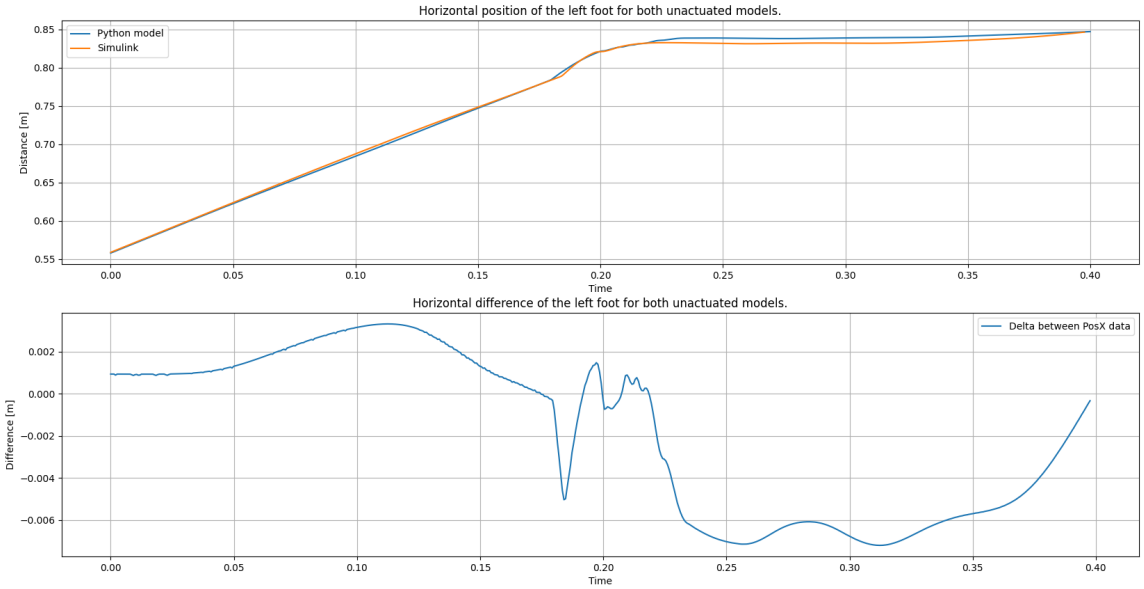

Figure 2.10: Ground contact for the left foot of unactuated models

It should also be noted that mistakes in the implementation may as well still be present and influence the behavior. As these influences couldn't be fully addressed or measured, a reflex adaptation method was employed to mitigate these divergences, as detailed in the following section.

Chapter 3

Model specific reflex adaptation

3.1 Introduction

3.1.1 Biological basis

A bipedal model or a person is able to match different biomechanical metrics (i.e., speed) by adapting its gait [26]. The importance of reflexes on the walking gait has been demonstrated by E. Paul Zehr and Richard B. Stein [27], stating "*reflexes function during human locomotion to preserve balance and ensure a stable walking pattern throughout the step cycle*". Reflexes in this case are environment and target dependent; a patient will need different muscle activations to walk at different paces or in different environments (i.e., ground angle).

For example, an older adult's reflexes will be different from those of a healthy young patient, with a less aggressive target angle for the trunk to result in a slower and safer gait.

3.1.2 Scale of the challenge

The goal is to select a specific set of reflex parameters that will achieve a certain objective (e.g., walking for a certain duration, at a certain speed, without falling). The chosen set of reflexes has several interesting properties:

- Changes generally have cascading effects.
- Changes can have antagonistic effects, leading to the same biomechanical properties for multiple sets of reflex.
- The reflex values are continuous and sometimes theoretically possible over an infinite range.

- Biological beings tend to conserve as much energy as possible in every action. In a walking context, this means that the optimal gait should minimize energy expenditure per gait cycle [28].

While the metabolic cost of a gait cycle can be estimated [29], it can not be guaranteed that the lowest point is reached, as it may only be a local minimum.

The problem to produce adapted controller for neuromusculoskeletal biped is described by Antonova et al. [30] as : non-convex, black box, non-linear and computationally expensive to run. This is reflected in this case since the execution time for a 10 seconds simulation is 10 minutes.The set of adaptable reflexes consists of 23 continuous parameters which will need to be estimated initially and refined through iteration.

3.2 Optimization method

The approach described here is largely based on the series of papers from R. Antonova et al. starting with "Sample Efficient Optimization for Learning Controllers for Bipedal Locomotion" [30,31], which aim to find the most fitting controller for a 16-muscle biped neuromusculoskeletal model.

Based on their approach and with further improvements, a method was derived:

1. **Define a fitness function:** This will be a metric or a series of metrics that approximate the quality of the gait.
2. **Define early stop metrics:** These metrics are used to predict future falls or problems and save execution time.
3. **Define the parameter space:** This is the range of parameters that will be explored to find the best set of parameters.
4. **Use Bayesian optimization:** Apply Bayesian optimization within the specified range.
5. **Range adjustments:** Human supervision to allow for periodic parameters range adjustments if needed.

3.2.1 Fitness functions

Multiple types of fitness functions exist, each with their own advantages, disadvantages and required task knowledge [32]. In the case of the bipedal model, while precise data on human gait are readily available, the complexity of the problem and its unpredictable nature necessitate simplicity. The behavioral fitness function

type is the most suitable in this context. Citing Nelson et al. [32] "*Behavioral fitness functions are task-specific hand-formulated functions that measure various aspects of what a robot is doing and how it is doing it.* "In this case the fitness function should quantify how closely the current simulation matches the expected behavior of the target extracted from the literature, whether it be a healthy human, a pathological one or another model. Three metrics where used in combinations:

1. The distance between the model and the target speed. A closer match is prioritized. This is a penalizing metric.

2. The time alive without being cut off. The mechanics of cut-offs are described in section 3.2.2. Longer duration is better. This is an encouraging metric as it reflects improved fitness.

3. Muscle energy spent. To simplify, the total sum of force from each muscle is used to approximate the energy spent. This is also a penalizing metric.

These components are combined to yield a fitness score, with higher scores indicating better performance with 100 being the highest score theoretically attainable. This score represents the maximum output of the encouraging metric(s) with no output from any of the penalizing metric(s). The metrics are weighted judiciously to ensure that the time alive has a higher impact than the other two penalizing functions combined. This prioritizes survival duration in the fitness evaluation process.

It should be noted that the approximation of the energy spent using the force is not perfect. The energy is not directly equal to the force since in a kinematic viewpoint $Energy = Force * distance$ and no dimension of the distance is taken into account. While the choice of a muscle energy model can influence the choice of the parameters [33], this approximation allows us to quickly assess the validity of an approach without complex calculation.

3.2.2 Early cut-off metrics

These have multiple objectives:

- First, cut off the simulation if it predicts that the results would not be interesting (i.e., if the biped is stationary, there is no need to simulate it).

- Second, cut off if a fall will appear in the next few seconds. Since many parameter sets lead to failure in the first gait cycle, being able to cut them off early is very useful.

- Third, avoid unwanted behavior. If the only metric was the distance crossed, this could lead to unwanted behavior such as the biped simply tensing all its muscles to jump ahead [34].

To address this, the following rules were developed:

- The first and simplest one: Are the hip and trunk in a normal position? Using values found in [35] and later confirmed in the simulation, the simulation is halted if it deviates outside of the allowed area, saving computational time as the model would be collapsing in the near future.
- The second one addresses whether the model is advancing at a correct and steady pace. For this, a "window of allowed area" was implemented which takes the target speed (i.e., 1.3 m/s for a healthy gait) convert it into a distance using time and adds 30 cm to each side of the target value. The position of the hip is then monitored to see if it remains within the window. If not, it serves as an early termination of the simulation, saving time. The rationale for using a target window instead of a target speed is that, since the model's initiation is chaotic, the speed is unstable and nonlinear, thus a window is provided to account for the initial start or non-linear behavior. It will also help find behavior that are near region of interest by the Bayesian optimisation described in section 3.2.4.
- The angle of the foot when it touches and leaves the ground. An unusual angle is a very good indicator of a fall in the next few seconds.
- Additionally, a comparison between the current fitness score and the fitness score of the best candidate to date is implemented, with the same rationale of a window as in speed. If the current fitness score is too low compared to the fitness score of the best candidate at that point in the execution, the trial is ended.

If at least one of the rules is triggered, the trial is ended.

3.2.3 Reflex value

In the implementation, adaptable reflexes are defined by Geyer [17] in Fig 3.1.

TABLE I

REFLEX PARAMETERS AND THEIR TOLERANCE. GAINS G_m AND k_{bw} ARE NORMALIZED TO $F_{\mathrm{max,m}}$ AND THE BODY WEIGHT. OFFSETS $\ell_{\mathrm{off,m}}$ ARE SHOWN IN FRACTIONS OF $\ell_{\mathrm{opt,m}}$. PRESTIMULATIONS $S_{0,m}$ ARE 0.01 (NOT SHOWN) EXCEPT FOR THE STANCE VALUES $S_{0,\mathrm{VAS}}$ AND $S_{0,\mathrm{BAL}}$ OF THE VAS AND OF THE TRUNK BALANCE MUSCLES HAM, GLU AND HFL

	value	min ... max		value	min ... max
G_{SOL}	1.2	0.97 ... 2.17	θ_{ref}	0.105	0.017 ... 0.11
G_{TA}	1.1	0.55 ... 3.2	k_d	0.25	0.10 ... 0.75
$\ell_{off,TA}$	0.71	0.59 ... 0.80	k_{bw}	1.2	1.3 ... 5.0
G_{SOLTA}	0.3	0 ... ∞	ΔS	0.25	0.14 ... 1
G_{GAS}	1.1	0 ... ∞	G_{HAM}	0.65	0 ... 0.67
$S_{0,VAS}$	0.09	0.047 ... 0.71	G_{GLU}	0.4	0 ... 0.52
G_{VAS}	1.15	0.82 ... 13.5	G_{HFL}	0.35	0.17 ... 3
k_φ	2	0 ... ∞	$\ell_{off,HFL}$	0.6	0 ... 0.67
$\varphi_{k,off}$	2.97	2.71 ... ∞	G_{HAMHFL}	4	0 ... 100
$S_{0,BAL}$	0.05	0.01 ... 0.32	$\ell_{off,HAM}$	0.85	0.83 ... ∞
k_p	1.91	1.78 ... 22	k_{lean}	1.15	1 ... 5.7

Figure 3.1: Table of Reflex Parameters extracted from Geyer's paper [17]

Here is a brief rundown of each type of reflex:

- **Muscle-based gain (G)**: This is an internal factor that acts between stimulation and activation, dictating how much past activation of the muscle should influence its current stimulation.
- **Length Offset (l_{off})**: This parameter sets a baseline or threshold length for muscle activation, where the muscle reflex is triggered if the muscle length exceeds this value, helping to control muscle responses and maintain biomechanical stability during movements.
- **Angle-based gain (κ)**: This parameter influences how angular movements of joints affect muscle stimulation, dictating the degree to which changes in joint angles modify the activation of associated muscles.
- **Inhibiting target angle (ϕ)**: This parameter sets the desired or reference angle for joint positions, inhibiting certain muscle activation mechanisms if a threshold is not met.
- **Proportional target angle (θ)**: This parameter adjusts muscle activation proportionally to the deviation from a target joint angle, enhancing the precision of movements and stability in dynamic conditions.
- **Pre-stimulation (S_0)**: This parameter represents the baseline level of muscle activation before any reflex-induced changes, setting an initial state of readiness or tone in the muscle.

All the listed parameters are linked to the control of the model and not its mechanical specifications. They were found by Geyer for his specific model and extracted from a range he initially guessed using the best of his biomechanical knowledge. This means that for a novel implementation the value of each will change.
Without knowing the parameters that will yield the best candidate, ranges are defined to encompass that set. This is a challenging step that requires biomechanical knowledge from the researcher, as a range that is too wide will take too much time, while one that is too narrow will prevent a valid candidate from ever being found. Additional steps to facilitate the selection will be discussed in section 3.2.5.

3.2.4 Bayesian Optimization

Fundamentally, Bayesian optimization is a technique used to efficiently find the optimal parameters of a function in the least amount of try.

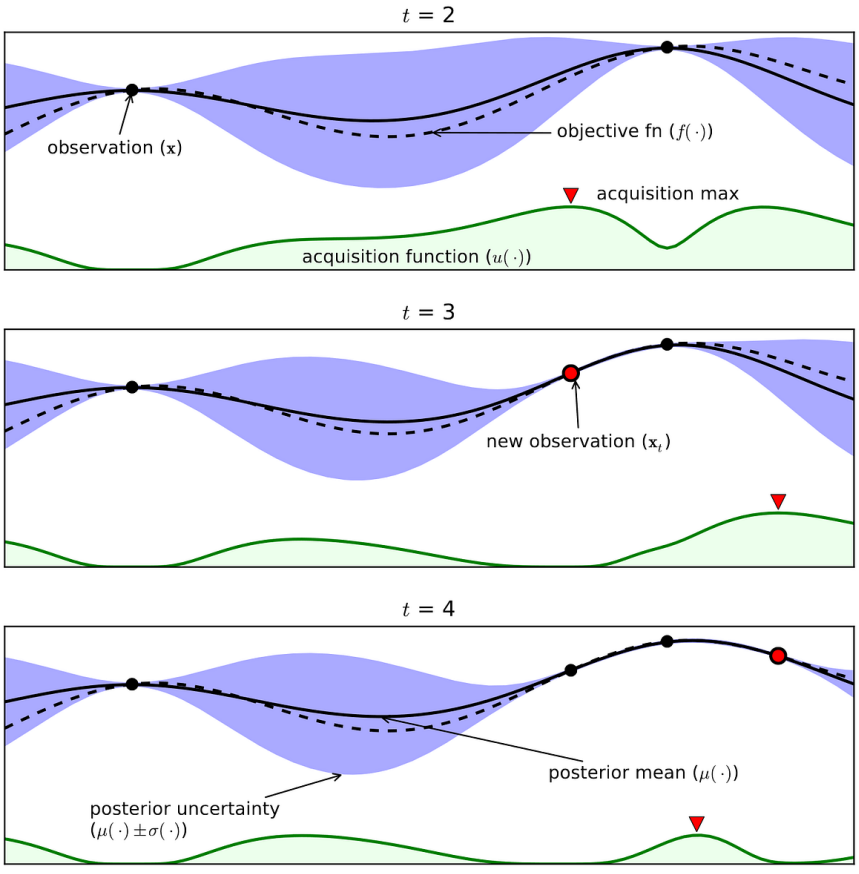

Figure 3.2: Illustration of Bayesian optimization process [36]

While Figure 3.2 illustrates the process in one dimension, the bipedal optimization problem typically involves a parameter space with 12 to 24 dimensions.

In Bayesian optimization, the base estimator and the acquisition function are two critical components that work together to efficiently explore the parameter space and identify the optimal set of parameters.

Base Estimator:

The base estimator, also known as the surrogate model, is a probabilistic model that approximates the objective function. It is used to predict the performance of different parameter sets without requiring expensive evaluations of the actual objective function. Commonly used base estimators include:

- **Gaussian Processes (GP)**: GPs are a popular choice due to their flexibility and ability to provide uncertainty estimates. They model the objective function as a distribution over functions, allowing for a probabilistic interpretation of predictions.
- **Random Forests (RF)**: RFs are an ensemble learning method that can handle high-dimensional spaces and non-linear relationships. They are less computationally intensive than GPs and can be more robust to noise.
- **Gradient Boosted Regression Trees (GBRT)**: GBRTs are an ensemble learning method that builds the model in a stage-wise fashion from decision trees. They are particularly effective for handling non-linear relationships and can provide robust performance in high-dimensional parameter spaces. [37]

The base estimator is trained on the observed data points and is continuously updated as new data is acquired. Its predictions are used by the acquisition function to guide the search for the optimal parameters. The initial paper by R. Antonova [30] used a Gaussian process as the base estimator, but through experimentation, this was found to be less optimal, as shown in Figure 3.3.

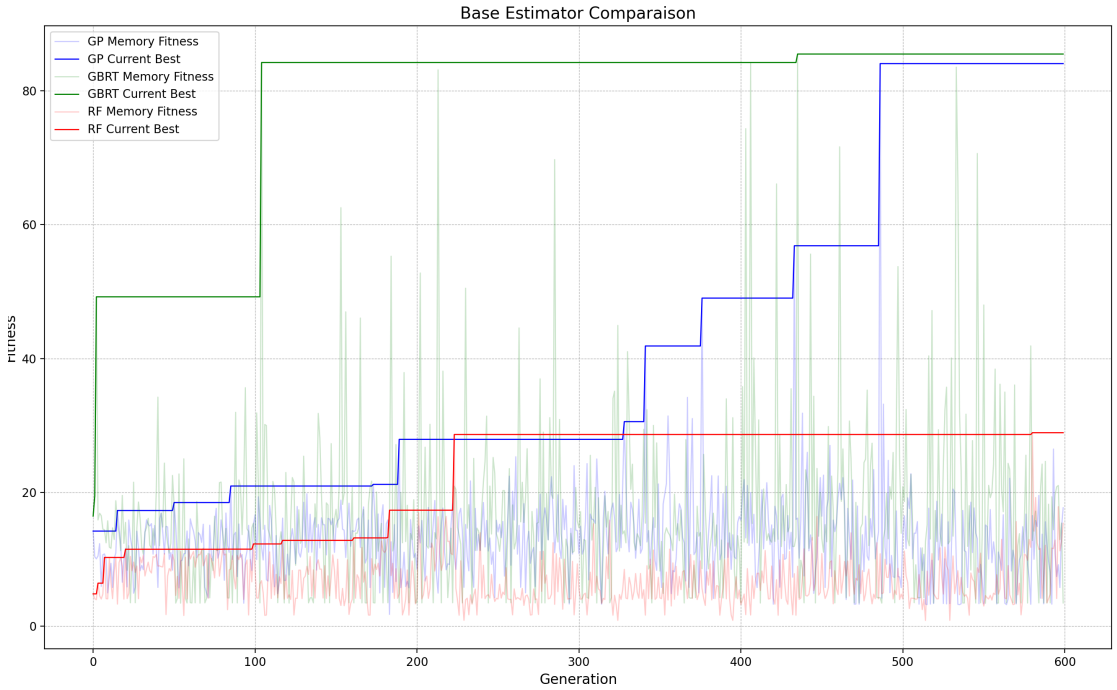

Figure 3.3: Base estimator comparison

This graph shows the fitness results of each trial and the current best candidate fitness for each base estimator. As a reminder, the higher the fitness the better, with 100 being a perfect score. All three estimators were asked to run a toy problem for 600 iterations. We can see that the GBRT base estimator (green) climbed at a faster rate and achieved an overall higher fitness. Due to the random nature of selecting a value in a large parameter space, the results of only one simulation per estimator are not highly significant but serve to demonstrate observed trends during the process. The GP process is also significantly slower than GBRT after the 200th trial. Between the 500th and 600th trials, the addition of new trials took 44.76% of the execution time, while the GBRT took only 7.23%. This alone could justify the selection of GBRT.

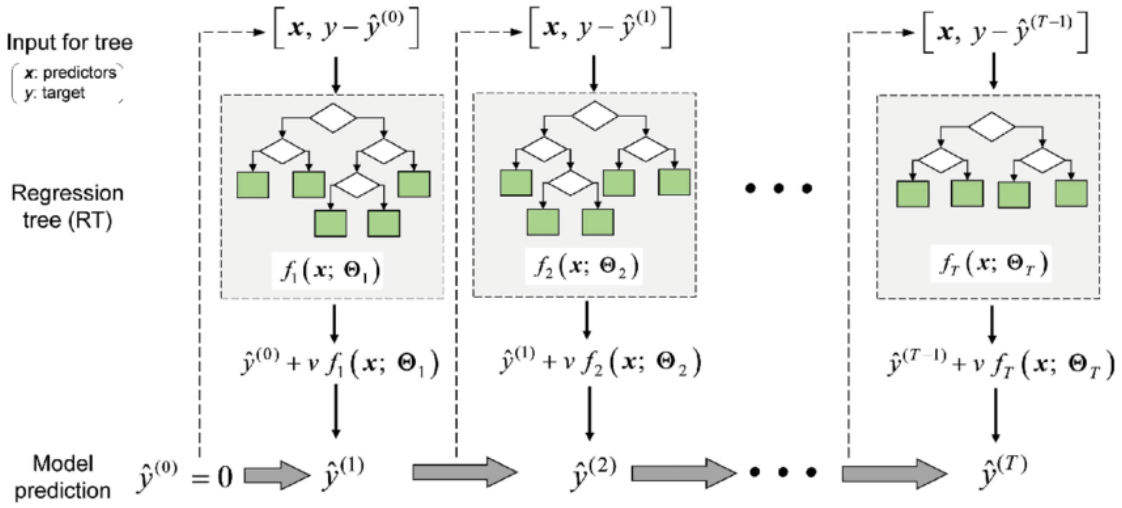

Figure 3.4: Gradient Boosted Decision Tree architecture [38]

The architecture of the GBRT (Gradient Boosting Regression Trees) shown in Figure 3.4 reveals a sequential ensemble learning method where multiple decision trees are built sequentially, with each tree correcting errors made by the previous one. This iterative process allows the model to learn complex patterns in the data by focusing on the residuals of the previous predictions. The final prediction is the sum of the predictions from all the trees, resulting in a powerful and accurate predictive model. [38]

Acquisition Function:

The acquisition function is a heuristic that guides the search for the optimal parameters by balancing exploration and exploitation. It quantifies the utility of evaluating a particular set of parameters based on the current model of the objective function. Commonly used acquisition functions include:

- **Expected Improvement (EI)**: This function estimates the expected improvement over the current best observation. It favors regions where the model predicts a high probability of improvement.
- **Probability of Improvement (PI)**: This function calculates the probability that a given set of parameters will improve upon the current best observation. It is simpler but can be less effective in some cases compared to EI.
- **Upper Confidence Bound (UCB)**: This function considers both the mean and the uncertainty of the model's predictions. It encourages exploration of regions with high uncertainty and exploitation of regions with high predicted values.

The choice of acquisition function can significantly impact the efficiency of the optimization process. It is often selected based on the specific characteristics of the problem being solved.

A similar experiment to the base estimator was conducted but this time confirming the method of R. Antonova [30] with the EI being the best choice.

3.2.5 Range adjustment

Each of the parameters will be explored within a certain range. This range must be fixed at some point but could be either too large, leading to excessive computation time, or too narrow, blocking possible candidates.

To avoid this, the range should be set up narrow to accelerate the initial search, with subsequent enlarging of the range if needed. To demonstrate this, the Figure 3.5 shows the data from a typical reflex adaptation process where the current reflex does not provide the desired performance and a new best candidate (higher fitness) is sought.

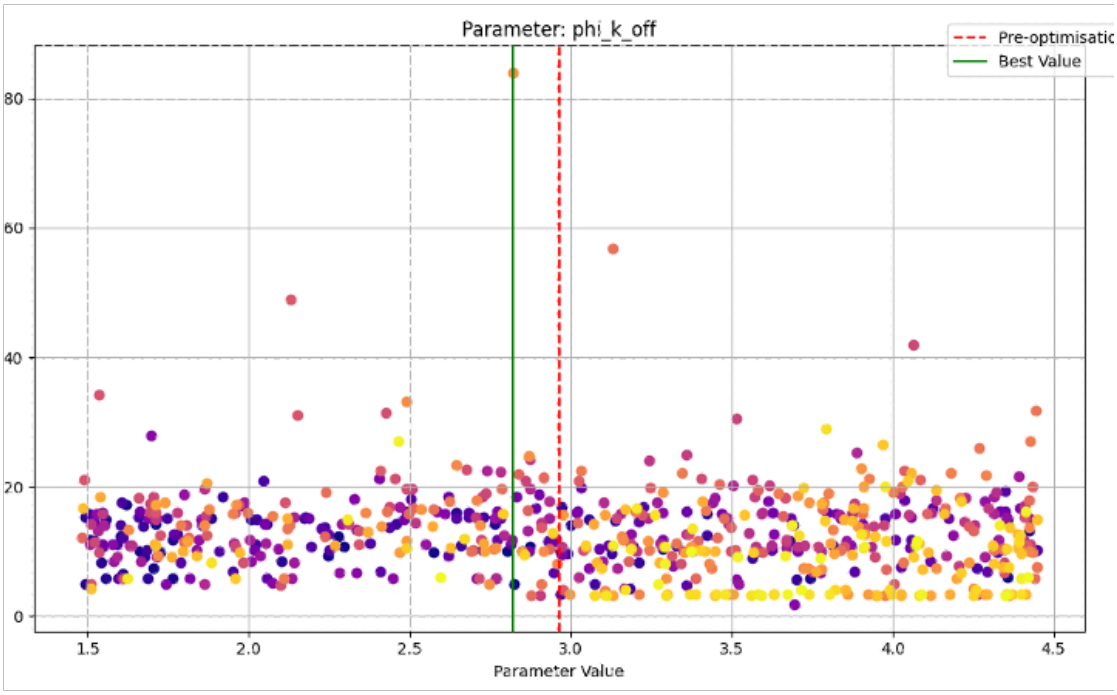

Figure 3.5: Parameter Ranges for Optimization

In this graph, each point represents the result of a trial with a given parameter value and its corresponding fitness. Of course this represents only one part of the combination of parameters, as can be seen in Figure 3.2.7. The lighter colors are

the most recent trials, while the darker ones are the first trials made. The green line represents the value of the best candidate, while the red dotted one is an optional value representing the value before the optimization.

The left graph shows a typical scenario where the original range appears to be correctly set, with no overall trend indicating that extending the range will bring any benefit.

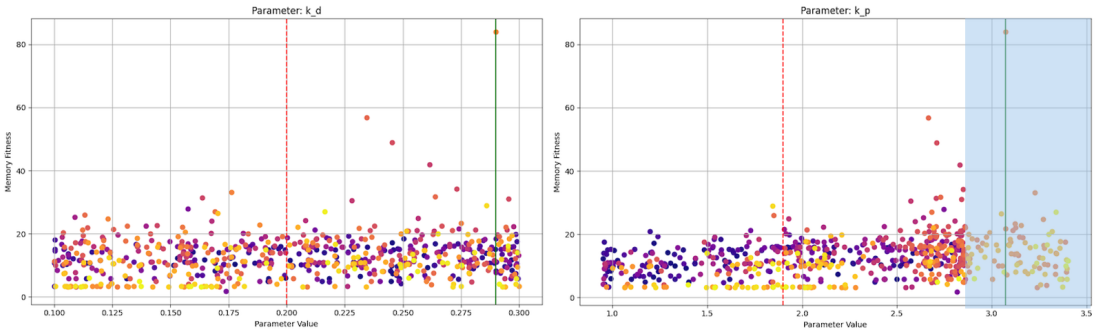

Figure 3.6: Parameter Ranges for Optimization

The right graph of Figure 3.5 represents a range extension that was beneficial, with the extension being colored in blue. The Bayesian algorithm also explored this additional range extensively, as visible by the number of lighter dots in the range and found the best current candidate.

The left graph is here to demonstrate a trend that would warrant a range extension.

The process of visualizing and extending the range was done during each reflex adaptation at various points, depending on the fitness progress. One optimization typically takes 8 to 10 hours.

Receding the range can sometimes be done if the data clearly shows that this region cannot be viable, but it is both a risk to accidentally reject valid candidates and the Bayesian algorithm tends to visit those regions less in favor of more promising regions.

3.2.6 Selection of a valid candidate

Since the score of 100 will realistically never be achieve, there arise the question of when to stop looking for a better candidate.

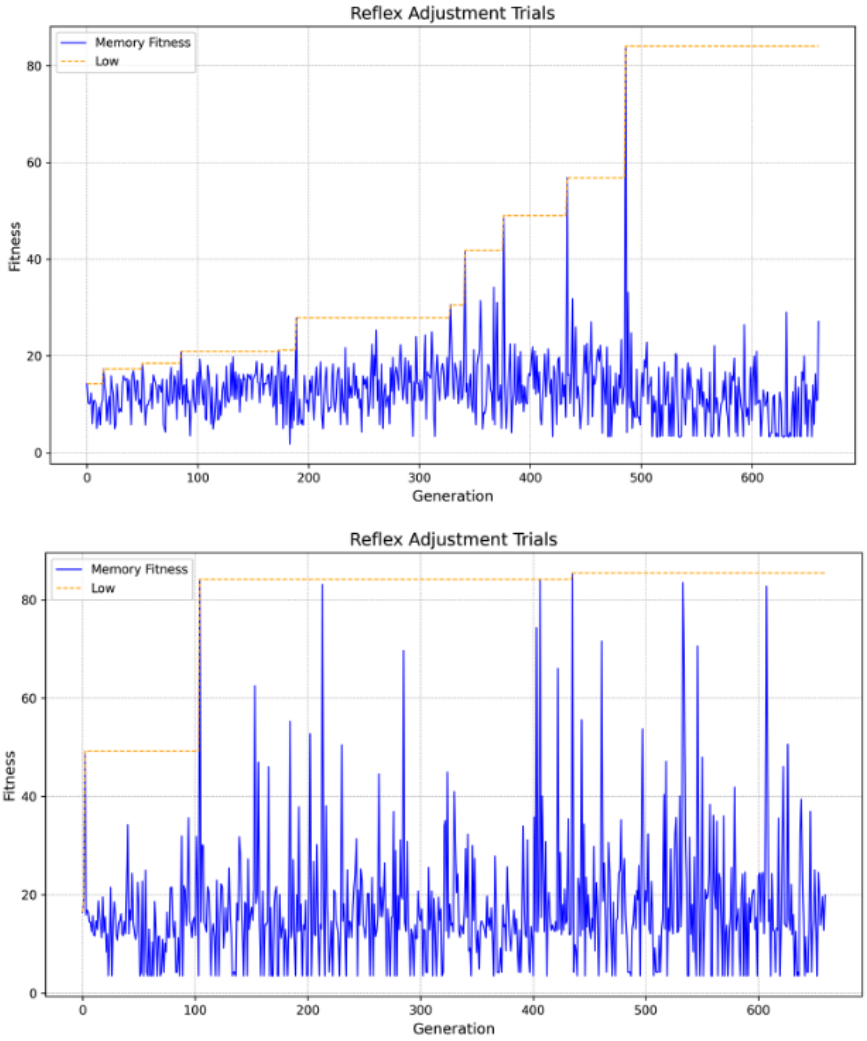

Figure 3.7: Example reflex adjustent trials

The Figure 3.7 illustrates the fitness results and the current best candidate in yellow for each trial during two example optimizations. This highlights the complexity of determining when to stop the optimization process. In this scenario, one optimization converged quickly to a solution, while the other did not. The fitness score is also highly dependent on the metrics and problem set up so relying on a number to reach is often pointless. Typically, experience dictates if the current best candidate is not beaten in the last 30% of the trials, it is unlikely that a significantly better one will be found in the future. However, this decision is highly dependent on randomness and is ultimately left to the researcher's judgment.

3.2.7 Validation

To validate the approach, the method was used on the first steady-state Python version. Wide ranges surrounding the exact parameters were defined, with the fitness functions being adapted to the specifics of the Python version. The objective was to find the original parameters back so the target was to have the same pace and energy consumption as the first steady-state Python version. The penalizing and disqualifying functions were also adapted accordingly.

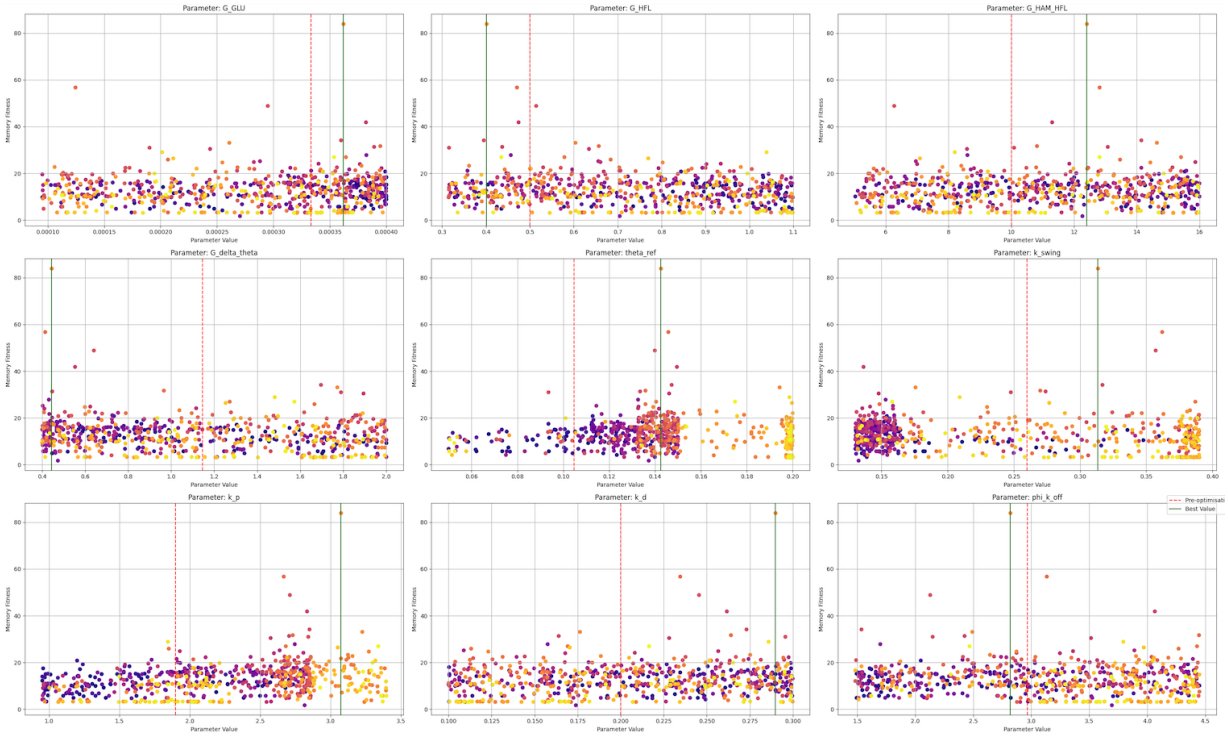

Figure 3.8: Validation Results of the Optimization Process

The results of the 1000 trials executed are shown in Figure 3.2.7. For ease of visualization, only the 9 of the 21 parameters are plotted. The metrics attained were comparable to the objective, as summarized in Table 3.1.

Table 3.1: Comparison of Objective and Attained Metrics

Metric	**Objective**	**Attained**
Speed (m/s)	0.913	0.911
Expended Energy	100%	92%

The reflex values found (in green in Figure) were different from the original

values (denoted in red). This indicates that for a bipedal controller, multiple sets of reflex parameters can yield similar biomechanical metrics.

The close match in speed and the reduction in expended energy demonstrate that the method is effective in adapting reflex parameters to achieve the desired performance.

Chapter 4

Results

4.1 The second steady-state Python version

4.1.1 Reflex adaptation

The nearly direct implementation of the Simulink version in Python resulted in a bipedal model with a visually correct gait but lacking in specific metrics such as speed. To resolve this, the reflex parameters were optimized following the method described in the section 3 to obtain the specific speed of 1.3 m/s. The optimization process lasted for 1000 trials and resulted in a model with the expected walking speed.

The Figure 4.1 shows the results of the 1000 trials optimization method that allowed the model to speed up and match the 1.3 m/s metrics. While the relationships between the reflex values are complex and non-linear, it is interesting to see that some general trends can be deduced from the values that changed the most.

The values that gained or lost a significant percentage of their original value are:

- **G_Vas:** The gain in the vastus. This muscle is mainly responsible for the extension during the swing phase; a higher gain leads to a quicker extension.
- **G_Gas:** The gain in the gastrocnemius. Responsible, along with the soleus, for the sagittal push exerted by the ball of the foot on the ground.
- **G_Ta and G_Sol_Ta:** A complex relationship that can be summarized as a feedback loop ensuring that the soleus and tibialis anterior (TA) are balanced. As the input from both the tibialis and nearby gastrocnemius drastically changes, the equilibrium will be altered.

Figure 4.1: Reflex Adjustment Process

- **G_HFL:** The hip flexors are responsible for the thigh swing speed; an increase in gain will lead to quicker and/or longer swings.
- **Theta_ref:** The objective angle for the trunk; a higher value will cause the model to lean more forward, resulting in a quicker gait.
- **K_swing:** Another complex relationship between two antagonistic muscles, the gluteus and hip flexors. Since one changed significantly, the relationship is affected.

4.1.2 Biomechanics comparison

Speed

The objective of the optimization was to match the expected speed with the lowest energy expenditure possible. This was achieved quite gracefully, as can be seen in Figure 4.2.

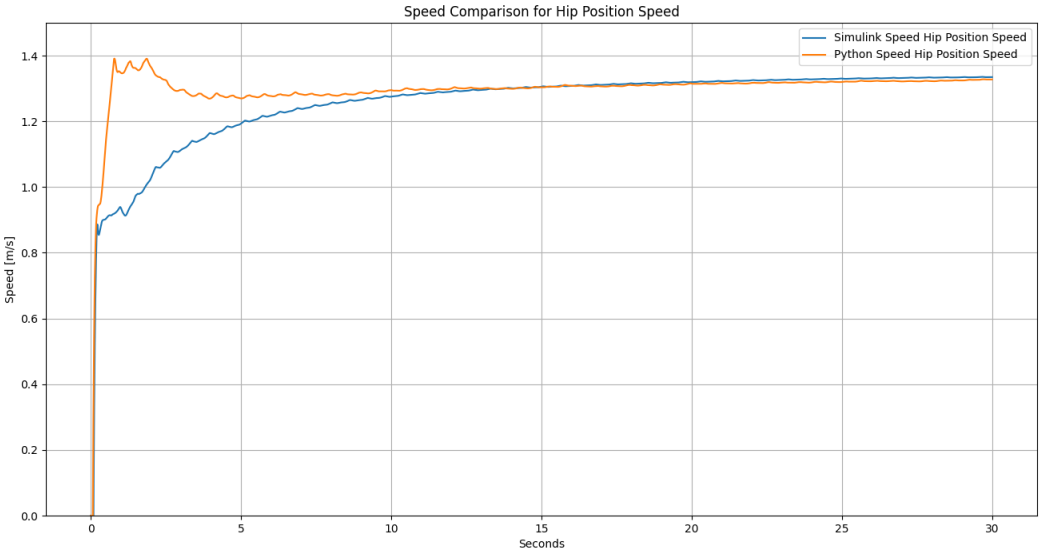

Figure 4.2: Speed comparison between Simulink and second steady-state Python version.

The hip position is used to determine the speed. While subject to slight oscillation, as can be seen in the 0-10s range, it is the most steady point on the biped, leading to the most accurate speed deduced solely by the position of a point. The starting conditions, such as leg and knee angle, were the same for both models.

However, since the ground reaction force in the Python model appears to be more slippery, this leads to the chaotic starts of the Python model. The model was selected by the Bayesian optimization to match the specified metrics only. Any other considerations are secondary and will lead to discrepancies such as this.

HFL stimulation

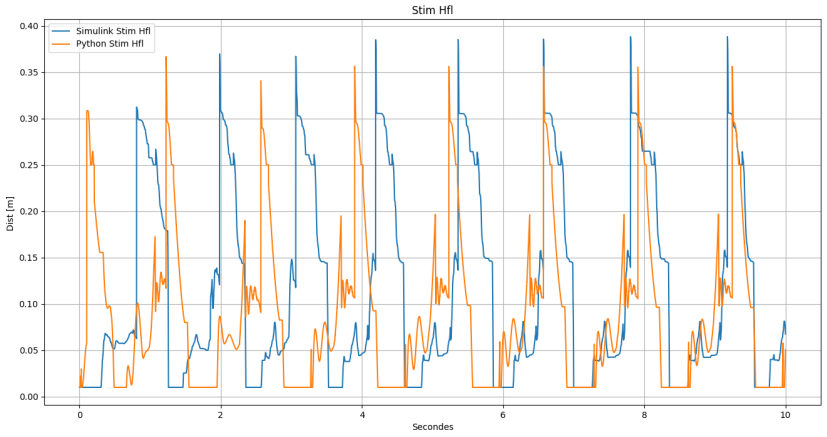

Figure 4.3: Comparison of HFL Muscle Stimulation

The Figures4.3 graph compares the HFL muscle stimulation between the models. This is part of a muscle system that is not selected by the optimization technique and it shows that while mostly similar, non-optimized biomechanics can diverge freely.

Gait frequency

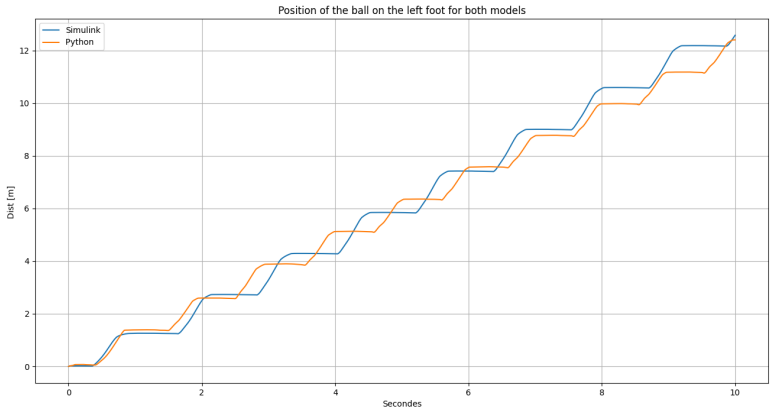

Figure 4.4: Position of the ball on the left foot for both models

The analysis of the position of the left foot through time allows for an analysis of the gait frequency. The Simulink model has a gait frequency of 51 cycles per minute, while the Python model is at 55.8 cycles per minute.While they are different from each other, they both fall within the range described as a normal stride rate of 54 ± 3.1 in "Mechanical power and efficiency of level walking with different stride rates" [39].

Kinetics and kinematics

In his paper, Geyer [17] compared the model perfomances to values from human patients as described in "J. Perry, Gait Analysis: Normal and Pathological Function" [40]. This section will compare those values to the second Python version to determine if they match both the original Simulink implementation and human patients.

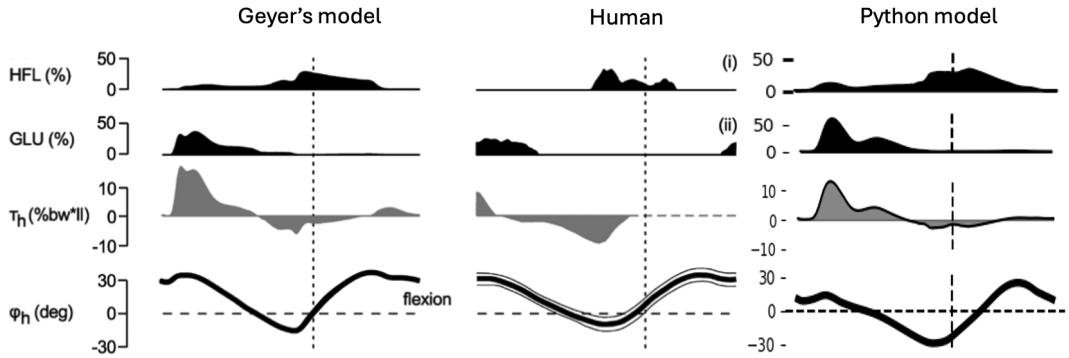

Figure 4.5: Comparison of Hip Movement in Geyer's model [17], Human reference [40] and Python Model

The plots in Figure 4.5 are a comparison of key values as a function of the stride progress. We can see that while the values are broadly similar, the range and fine points differ.The first two lines are activation values for antagonistic hip-linked muscles. It is interesting to see that Geyer's model and the Python model share similarities in HFL that are different from the human values. Simulation and modeling often lead to a loss of precision against the target.The third line shows the torques acting on the hip as a percentage of body weight. The same conclusion applies here.The last line represents the hip angle. The most glaring difference is a lower hip angle at the end of the stride. This can be explained by the Python model having a higher step frequency and a reference angle for the torso closer to 15°.

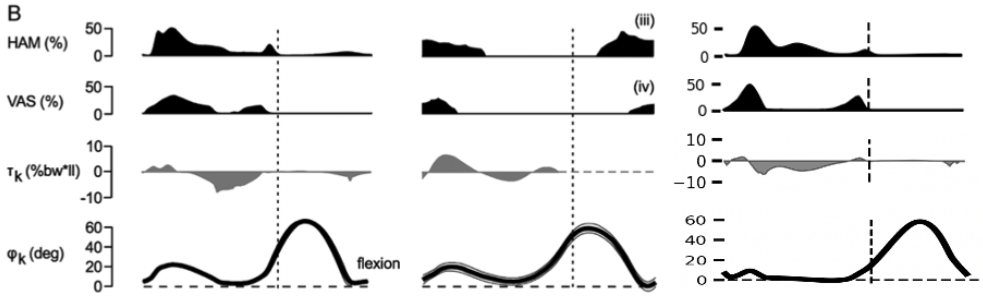

Figure 4.6: Comparison of Knee Movement in Geyer's model, Human reference and Python Model

Once again, the similarities are more marked between the Simulink and the Python models than with the human model. The vertical dotted line at 60% indicates the suggested "toe off" (moment when the toes leave the ground) position.

It appears to be different in the Python version, leading to inaccuracies in this region. The toe off is later in the Python model, which is compensated by a faster speed during the swing phase.

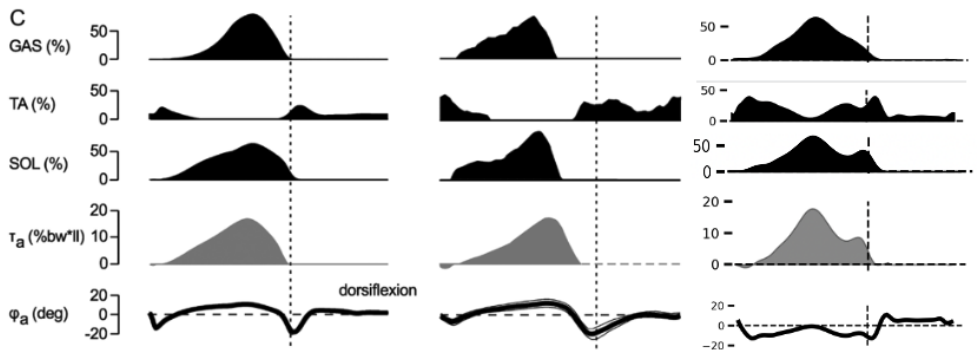

Figure 4.7: Comparison of Ankle Movement in Geyer's model, Human reference and Python Model

The ankle joint seems to be the most diverging part of the model, with the early toe off having the most effect. As seen in Figure 4.1, the plantar flexion-linked muscle gains have massively increased. This leads the model to stand on its toes earlier than expected, resulting in the vastly different ankle behavior seen in Figure 4.7.

Conclusion

The goal of this section is to demonstrate that the neuromusculoskeletal biped adapted from Geyer's implementation can be used as a basis for future work without losing its foundational integrity. Significant efforts were made to ensure that the second steady-state Python model achieves the target speed through optimization. While there is some loss of accuracy in finer biomechanical metrics, as is common in any model adaptation, the overall usefulness and applicability of the model remain intact. This model still provides a robust platform for further research and development in gait analysis and assistive device optimization.

4.2 Pathological study: Aging

4.2.1 Introduction

The impact of aging on the body is well-documented, with a significant focus on the increased fall risk associated with it [41]. Various approaches, such as collecting data directly from patients [42], are used to draw conclusions from gait analysis.

Aging leads to changes in biomechanical propreties of the body and brain both of which can significantly impact gait [43]. Detailed biomechanical gait analysis can identify specific age-related changes in gait patterns, aiding in the development of targeted interventions to mitigate fall risks and improve the quality of life for the elderly.

This section will utilize previous results and methods to simulate an aged gait. The goal is to facilitate easier, safer and faster analysis of aged gait, ultimately aiding in the development of assistive devices to prevent falls.

4.2.2 Biomechanical Changes with Aging

Aging induce a change in muscle mass and composition that is called sarcopenia, which begins around age 50 and becomes more prevalent by age 60 [44, 45].

This muscle loss is caused by decreased protein synthesis and increased proteolysis and it contributes to chronic diseases, physical inactivity and malnutrition [46]. Such alterations can lead to a more cautious gait pattern, characterized by shorter stride length and increased double support time [5, 47].

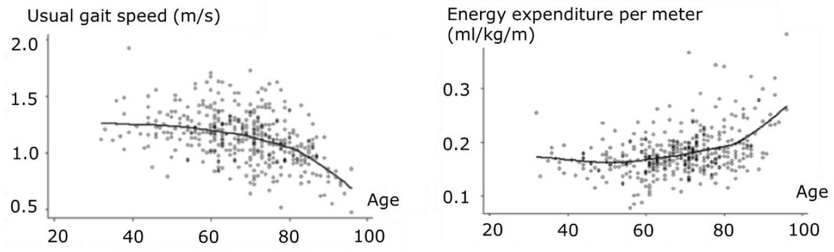

Figure 4.8: Change in speed and energy expenditure [5]

This cautious gait will lead to a slower and more expensive gait as seen in Figure4.8.

Modeling the impact of aging on neuromuscular control

The studied neuromusculoskeletal biped use a hill model for muscular simulation as can be seen in the section 1.3.2. The paper "Adjustment of Muscle Mechanics

Model Parameters to Simulate Dynamic Contractions in Older Adults" by Darryl G. Thelen [48] propose a way to adjust parameters of Hill-type musculo-tendon models to reflect age-related changes in muscle mechanics between ages 30-70.

	τ_{deact} (ms)	$V^{M}_{\max}$ (L^{M}_{o}/s)	ε^{M}_{0}	$\overline{F}^{M}_{len}$
Young	50	10	0.6	1.4
Old	60	8	0.5	1.8

τ_{deact}-deactivation time constant, $V^{M}_{\max}$-maximum muscle contraction velocity expressed in optimal fiber lengths (L^{M}_{o}) per second, ε^{M}_{0}-passive muscle strain due to maximum isometric force, $\overline{F}^{M}_{len}$-ratio of maximum lengthening muscle force to isometric force.

Figure 4.9: Illustration of constant parameter changes in the Hill model to simulate aging effects [48].

The key changes made to the Hill-type muscle model parameters to represent aging effects between 30 and 70 years old were:

1. Maximum contraction velocity (V^{M}_{max}): Decreased from 10 to 8 optimal fiber lengths per second, a 20% reduction, to reflect slower contraction speeds in older muscle.

2. Maximum normalized force during lengthening contractions ($\bar{F}^{M}_{len}$): Increased from 1.4 to 1.8 times isometric force, as older muscle exhibits less of a strength deficit during lengthening.

3. Passive muscle strain due to maximum isometric force (ε^{M}_{0}): Reduced from 0.60 to 0.50 to represent the relative increase in passive muscle stiffness with age.

4. Muscle deactivation time constant (τ_{deact}): Increased from 50 to 60 ms to account for slower calcium uptake by the sarcoplasmic reticulum in older muscle.

5. Maximum isometric muscle forces (F_{Max} in Python): Reduced by 30% to account for the loss of muscle mass and specific strength with age.

The proposed changes where adapted and used in the implementation with some difference as for example the muscle deactivation time constant is set by Geyer to 0.01s which is lower than the proposed value for young patient in the

Figure 4.9. In these cases a ratio was implemented at the relevant place to obtain the same effect as described in Thelen's paper [48].

To demonstrate the effect of the implementation of these parameters, two simulations using the muscle modules from the main implementation were executed.

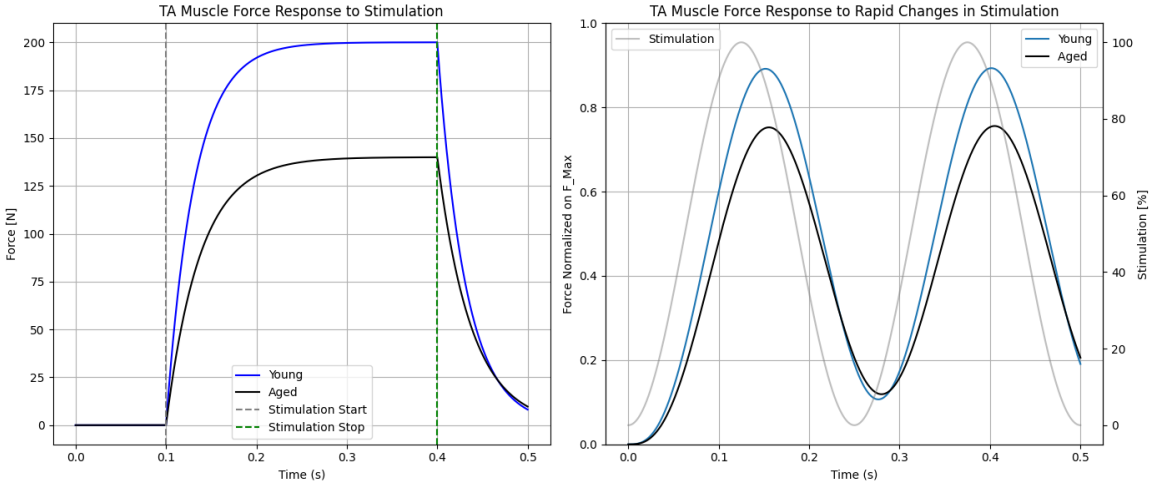

Figure 4.10: Simulation results showing the impact of aging on muscle force response. The graph compares the muscle force response to stimulation in young and aged muscle models.

The graphs in Figure 4.10 present a comparative analysis of simulated muscle force responses between young and aged muscle models in the python implementation using the Tibialis (TA) values as an example.

Muscle force response to fixed stimulations

The left graph illustrates the simulation of muscle force response to a single stimulation event. The x-axis represents the time in seconds, while the y-axis indicates the muscle force in Newtons.

Young Muscle Model: The force response in the young muscle model (blue line) shows a rapid increase in force following stimulation, reaching a peak quickly and then gradually declining after the stimulation stops. This behavior is indicative of the higher contraction velocity and lower passive stiffness in younger muscles.

Aged Muscle Model: In contrast, the aged muscle model (orange line) exhibits a slower rise in force, a lower peak force and a more prolonged decline. These trends are consistent with the reduced maximum isometric muscle forces, decreased contraction velocity and increased passive stiffness associated with aging.

Muscle force response to rapidly changing stimulations

This graph illustrate the simulated response to a sinusoidal stimulation signal, the y-axis is in force normalized on F_max to allow finer comparison between profile.

Young Muscle Model: The force response in the young muscle model (blue line) follows the rapid changes in stimulation (grey line) more closely, demonstrating a higher responsiveness and quicker adaptation to changes in stimulation levels.

Aged Muscle Model: The aged muscle model (orange line) shows a delayed and dampened response to the rapid changes in stimulation. The force generated is lower and the muscle takes longer to adapt to the changes in stimulation levels.

Conclusion: The implementation of an aged effect on muscle is consistent with the paper: "Adjustment of Muscle Mechanics Model Parameters to Simulate Dynamic Contractions in Older Adults" [48].

4.2.3 Reflex Adaptation

The first steps of this method is to define the fitness function to ensure that we are optimising for the right objective.

The paper from Darryl G. Thelen [48] on which the aging process is based, recommends a speed of 1.0 m/s for older adult aged 70+, this is corroborated by multiple other studies [48, 49].

While those sources recommend a 1.0 m/s walking speed for patients aged 70+, multiple others [50–52] suggest a preferred walking speed of 1.3 m/s for the same age brackets.

The paper "Systematic review and meta-analysis of gait mechanics in young and older adults" by Boyer et al. [53] provides a comprehensive review of various studies on biomechanical changes in older adults by analyzing a pool of 29 relevant papers, out of which only 5 analysed a speed closer to 1.0 than 1.3m/s

Paper	Sample size		Age (years)		Speed (m/s)		Step length (m)		Controlled speed (m/s)	
	Young	Old	Young	Old	Young	Old	Young	Old	Young	Old
Average (SD)	19.8 (11.3)	17.9 (10.9)	27.2 (2.1)	71.6 (3.3)	1.32 (0.10)	1.36 (0.19)	0.70 (0.06)	0.64 (0.08)	1.28 (0.14)	1.28 (0.17)

Figure 4.11: Summary of the age and speed characteristics of the participant to the review from Boyer et Al. [53].

This paper will be useful to quantify the validity of our approach. As can be seen in Figure 4.11, the review aimed at participants who were either young or older adults in the target age range. The average preferred walking speed for the older cohort is 1.36 m/s.

Since the work of Darryl G. Thelen [48] proposed a specific solution the aging process but suggests a speed different than most analysis of the aged gait, two separate models will be developed and analysed in parallel.

The aged 1.0 m/s version

The method described in the chapter 3 was applied, yielding the results shown in Figure 4.12.

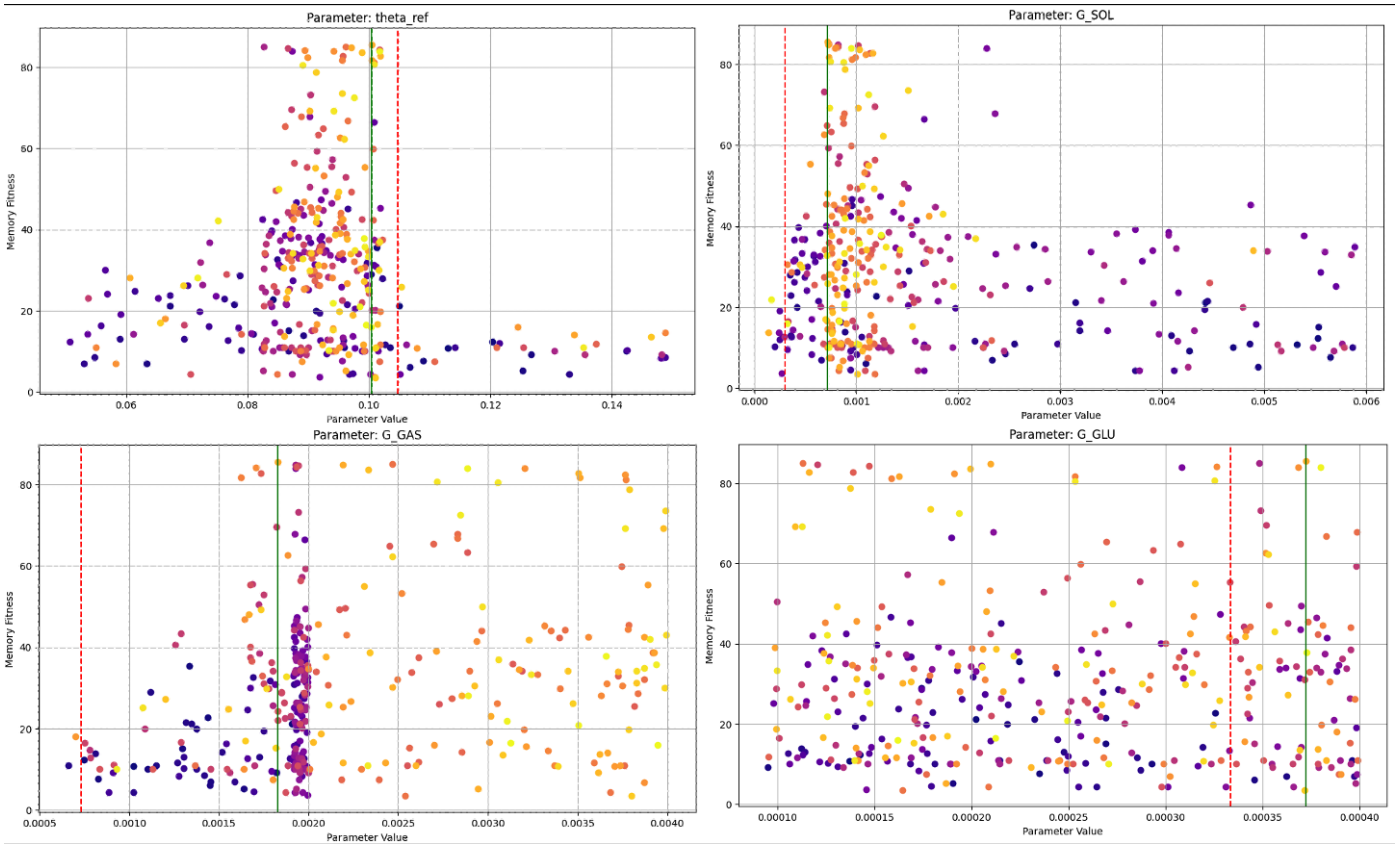

Figure 4.12: Results of the reflex optimization for the 1.0 m/s aged version

For clarity, only 4 of the 21 parameters are shown in Figure 4.12. The target speed of 1.0 m/s was achieved efficiently, with a fitness score ceiling around 85-90, which was reached both early (indicated by darker data points) and frequently. This can be explained by the original bipedal model values (shown in red) already being close to the target speed, requiring minimal adjustments.

The θ_ref parameter dictates the desired angle of the trunk; a lower value results in a more upright posture, which is consistent with the expected behavior

in older adults [54]. The lower left graph is interesting because, although the range extensions appeared promising, they did not yield better fitness results. The lower right graph shows that the G_Glu parameter seems to have a small impact on the final results. This could be due to its range being comparatively small relative to its impact or because it easily combines with other parameters.

The aged 1.3 m/s version

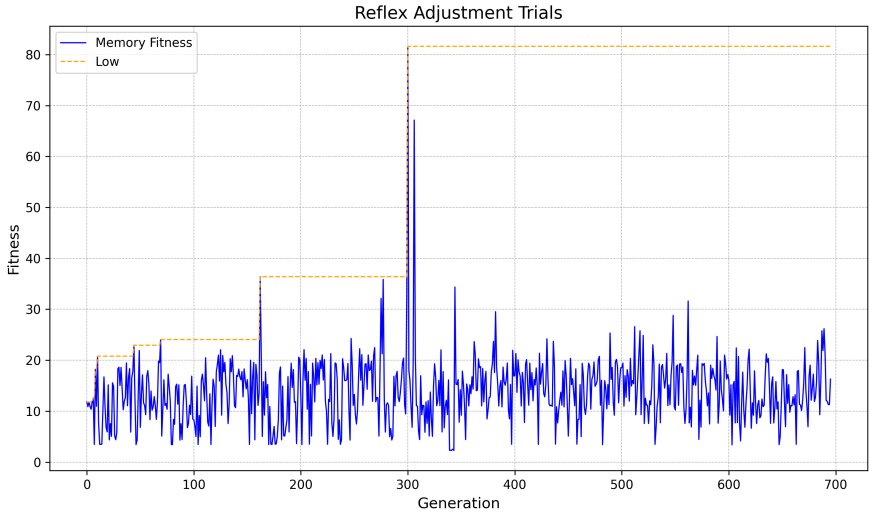

Figure 4.13: Results of the reflex optimization for the 1.3 m/s aged version

As shown in Figure 4.13 the optimization yielded less numerous valid candidates for the 1.3 m/s condition. This can be explained by the difficulty to reach a higher speed with less powerful and less responsive muscle.

4.2.4 Results and interpretations

The goal of this section is to evaluate whether the reflex adaptation method described in Chapter 3 results in biomechanical performances that accurately depict the mechanics of pathological gaits. This assessment involves comparing the healthy version of the second steady state with the pathological implementations. The choice to directly compare the aged versions to the second steady state rather than using biomechanical values from the literature is intended to minimize potential noise or inaccuracies in the current implementation by focusing on the effects introduced by the aging process. An alternative approach would have been to assess the

pathological versions against data from studies on aged gait, but discrepancies could have stemmed from limitations in the base model implementation as well.

The Table 4.1 resume the three version origin and specificities.

Metric	**Young**	**Old 1m/s**	**Old 1.3m/s**
Speed (m/s)	1.3	1.0	1.3
Step frequency (steps/s)	0.92	0.77	0.89
Step length (meters)	1.42	1.30	1.46
Origin	Second Steady state	Aged adaptation	Aged adaptation

Table 4.1: Comparison of basic metrics between versions

For this section, we referenced the paper "Systematic review and meta-analysis of gait mechanics in young and older adults" by Boyer et al. [53]. This comes with some remarks:

- The analysis uses wording directly from the paper by Boyer et al., such as "Young more extended than older," which may be unclear but is extracted directly from the review for accuracy's sake.
- The term "Power Generation/Absorption" has been determined to mean peak hip power generation, as it would otherwise refer to energy generation.
- Flexion/extension Moments are also treated as peak torque in the according direction.

All analyses were done on 60 seconds of data from each version. The number of gait cycles was not consistent across versions stemming from different speed and gait frequency, but this was accounted for. The first three cycles were removed since they often contain perturbations linked to the starting conditions and all analysis were made on the mean of the strides from each leg. The strides were adjusted to a percentage-based x-axis for compatibility.

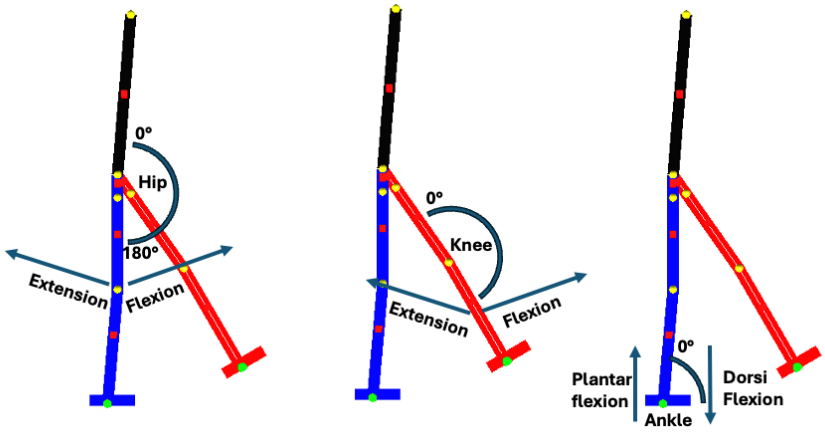

Figure 4.14: Illustration of the direction and calculation methods for hip, knee and ankle angles.

To facilitate understanding in the following sections, Figure 4.14 provides a visual representation of the direction and calculation methods for hip, knee and ankle angles. These angles are computed relative to other limbs, beginning at 0 and progressing clockwise. Torques and moments are determined using the same methodology as angles.

In the following sections, the kinematics and kinetics results for the hip, knee and ankle joints will be presented, comparing the metrics between the young and aged versions. These joints are involved in an intricate way in the specific biomechanics of the biped, making them interesting indicators to check the validity of the approach.

Hip Joint Kinematics and Kinetics Analysis

Table 4.2 presents the metrics from the review by Boyer et al. [53], comparing the values for the young version and using trends from Boyer et al. to analyze the performances of the aged versions. A green cell indicates a confirmed trend, while a red cell indicates the opposite.

Metric	Young	Trend	Old 1m/s	Old 1.3m/s
Kinematics				
Heel Strike Angle	134.82°	Young more extended than older	145.13°	135.23°
Peak Flexion	120.91°	Young more extended than older	131.63°	127.49°
Peak Extension	174.91°	Young more extended than older	183.44°	183.69°
Range of Motion	54.00°	Young ROM less than older	51.81°	56.20°
Kinetics				
Flexion Moment	-56.95 Nm	Young moment less than older	-79.13 Nm	-118.73 Nm
Extension Moment	262.56 Nm	Young moment less than older	121.81 Nm	246.4 Nm
Power Generation	513.45 W	Young power less than older	100.60 W	563.81 W
Power Absorption	-166.28 W	Young power greater than older	-79.93 W	-134.24 W

Table 4.2: Comparison of Hip Metrics Between Young and Older Adults

Aged 1.0 m/s: The kinematic trends of the hip are universally reversed, with this version consistently showing more extended hips, as seen in Figure **??**. This is likely due to the slower speed leading to a more upright trunk, a reduced need for aggressive forward steps and a smaller range of motion. The kinetics are more encouraging; the effects of aging are evident and even slower motions than the young version lead to higher power generation for flexion. However, the extension behavior, typical of a slow and cautious walker, results in lower power generation.

Aged 1.3 m/s: The kinematics align more closely with the expected trends, with the graph showing similarities to both other versions. The peak values of both aged versions align in percentage and degree, while the overall profile matches the young version. This emergence of a pattern is encouraging. In terms of kinetics, the power generation aligns with expectations, with the only anomaly being the peak extension moment, which closely follows the Young version.

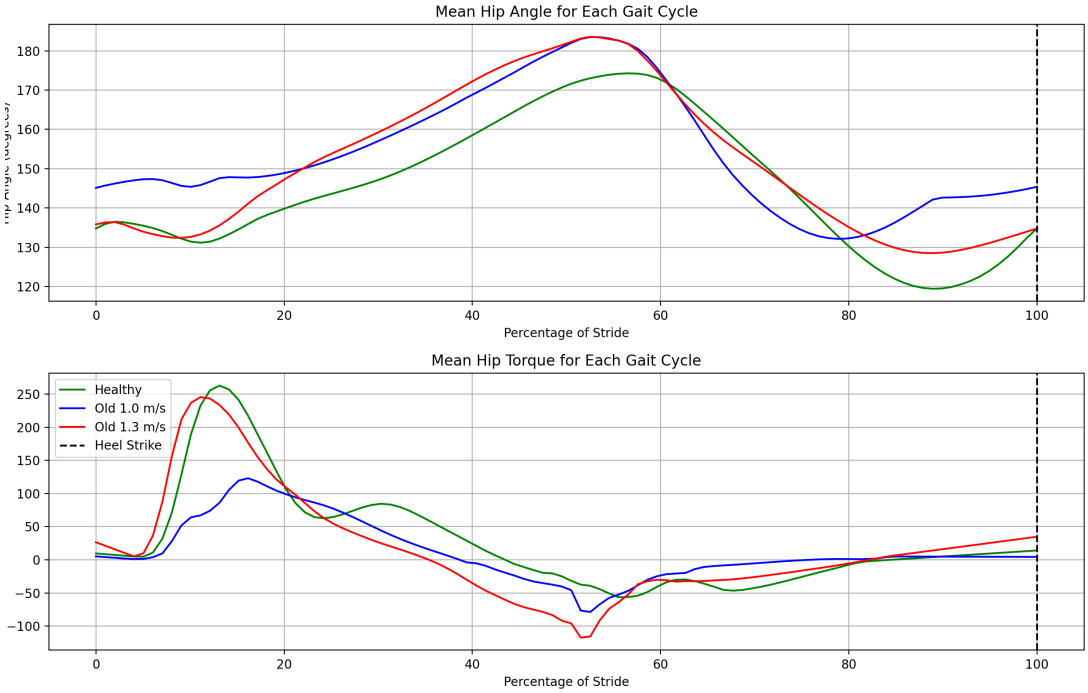

Figure 4.15: Hip metrics analysis for young and older adults.

Knee Joint Kinematics and Kinetics Analysis

Table 4.3 presents now the same metrics but for the knee. Again, a green cell indicates a confirmed trend, while a red cell indicates the opposite.

Metric	**Young**	**Trend**	**Old 1m/s**	**Old 1.3m/s**
Kinematics				
Heel strike angle	236.19°	Young more extended than older	223.43°	250.43°
Peak flexion swing	184.39°	Young more flexed than older	177.13°	186.07°
Range of motion	123.49°	Young ROM less than older ROM	111.74°	99.14°
Kinetics				
Flexion Moment	38.72 Nm	Young moment greater than Older	19.93 Nm	183.85 Nm
Extension Moment	-127.47 Nm	Young moment greater than Older	-103.79 Nm	-124.61 Nm
Power generation	1247.30 W	Young power greater than Older	444.29 W	1852.13 W
Power Absorption	-162.21 W	Young power greater than Older	-132.26 W	-234.51 W

Table 4.3: Comparison of Knee Metrics Between Young and Older Adults

Aged 1.0 m/s: The kinematics and kinetics show a perfect comparison, with

the kinematic trends from Figure 4.16 indicating a match in profile with a more flexed knee. This is consistent with a more efficient slower gait since maintaining the knee at an angle under load is costly.

Aged 1.3 m/s: The main theme is a less efficient and more abrupt walk. The particular spike seen at the start of the torque graph in Figure 4.16 seems to stem from the angle at which the knee is during heel strike. The more extended knee takes a higher torque to stabilize. Additionally, the longer time between toe-off and heel strike suggests a longer time to gather speed from gravitational acceleration, possibly causing the strike angle to be less flexed than it should be. Once again, the aged 1.3 m/s version mimics parts of both graphs.

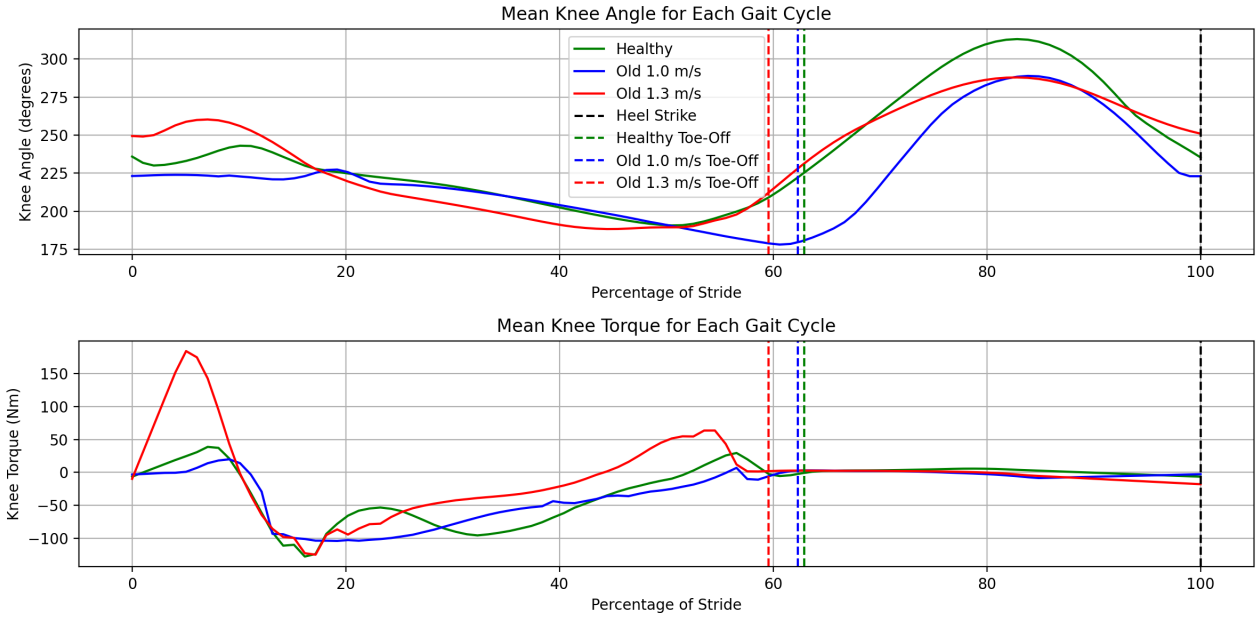

Figure 4.16: Knee angle and torque analysis for young and older adults.

Ankle analysis

Metric	Young	Trend	Old 1m/s	Old 1.3m/s
Kinematics				
Heel strike angle	95.29°	Young more dorsiflexed	98.07°	81.64°
Toe-off angle	101.45°	Young more plantar flexed	102.00°	114.96°
Peak plantar flexion angle	17.99°	Young more plantar flexed	23.89°	14.76°
Range of motion	92.37°	Young greater ROM	89.74°	79.70°
Kinetics				
Dorsiflexion Moment	-7.15 Nm	Young moment greater	-4.94 Nm	-2.91 Nm
Plantar Flexion Moment	124.59 Nm	Young moment lower	117.14 Nm	99.61 Nm
Ankle Power Generation	158.14 W	Young power lower	224.78 W	594.07 W
Ankle Power Absorption	-222.29 W	Young power greater	-333.15 W	-292.00 W

Table 4.4: Comparison of Ankle Metrics Between Young and Older Adults

The figures 4.17 and table 4.4 reveal insights into the kinematics and kinetics of the ankle joint.

The aged 1.0 m/s version performs well on several metrics, likely due to its slower, more conservative gait. The slower speed allows for a more optimal ankle angle at heel strike, with toe off occurring around 180°. This strategy appears to conserve energy at slower speeds with aging.

The peak power generated is lower, fitting with the slower gait, but the smoother graph indicates less reliance on muscle changes and a more predictable, safer gait overall. These data points could lead to interesting research avenues.

The aged 1.3 m/s version relies more heavily on the ankle for propulsion, with higher power usage and absorption. The more extended ankle at heel strike puts extra strain on the joint, creating an abnormal rise in torque that is less energy efficient.

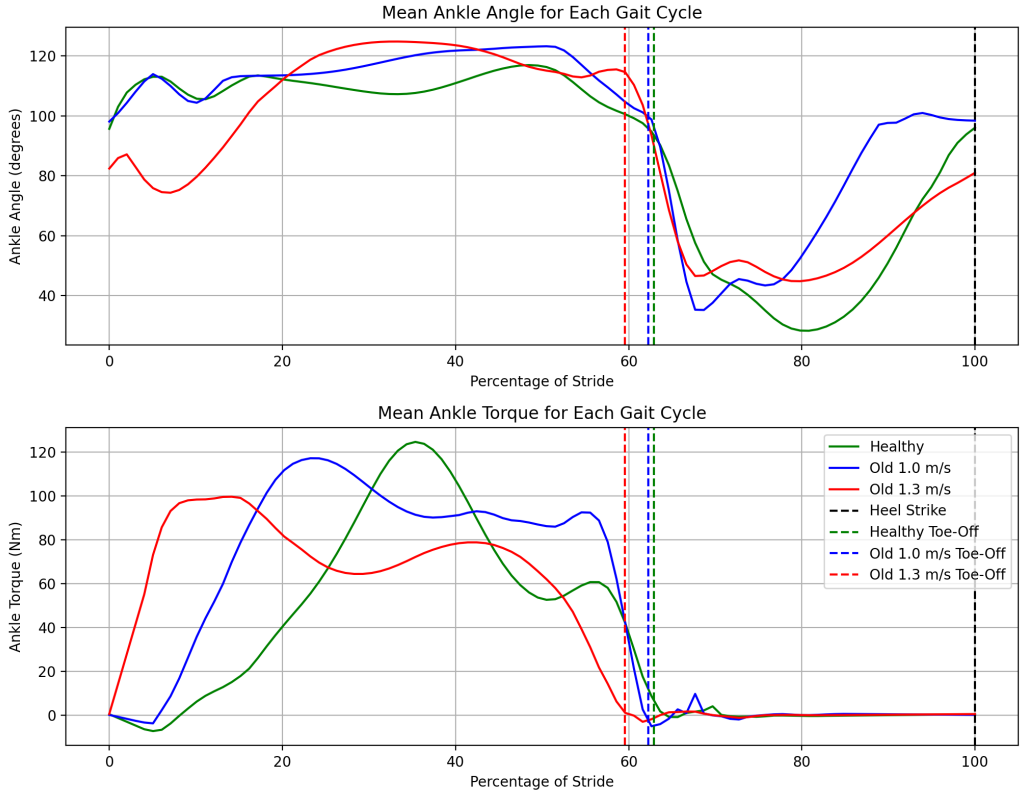

Figure 4.17: Hip metrics analysis for young and older adults.

Conclusion

The goal of this analysis was to determine whether our method can accurately predict the behavior of aged patients by comparing the kinematics and kinetics of hip, knee and ankle joints between young and aged versions. The findings reveal that while there are some promising aspects, the models do not closely match the expected behavior of aged patients, indicating significant areas for improvement.

The aged 1.0 m/s version demonstrates some alignment with the expected behavior of older adults, but it only passes 14 out of the 23 metrics from the review [53]. This version exhibits a more conservative and stable gait, characterized by more extended hips, a more flexed knee and an optimal ankle angle at heel strike. These kinematic trends are consistent with a cautious walking strategy aimed at minimizing fall risk.

However, the model's overly conservative approach may not fully capture the variability in older adults' gait patterns. The kinetics show higher power generation for flexion and lower power generation for extension, which are typical of a slow and cautious gait. Despite these positive aspects, the model's failure to meet

all expected metrics indicates that it does not fully predict the behavior of aged patients.
The aged 1.3 m/s version presents a more complex picture and passes only 12 out of the 23 metrics. While it shows some alignment with the young version in terms of power generation, it also highlights the challenges of maintaining efficiency at higher speeds in older adults.

The kinematics reveal a higher torque requirement during heel strike, particularly at the knee joint, due to a more extended knee angle. This suggests a shorter terminal swing after gathering more speed in the mid-swing, leading to a less flexed strike angle. The ankle joint in this version relies more heavily on propulsion, with higher power usage and absorption, resulting in an abnormal rise in torque that is less energy efficient. These findings indicate that while the aged 1.3 m/s model can mimic certain aspects of youthful gait, it also underscores the biomechanical limitations and inefficiencies that arise with aging at higher walking speeds. The model's primary issue is its inability to maintain efficiency, which could lead to increased fatigue and higher fall risk in older adults.

Overall, neither the aged 1.0 m/s nor the aged 1.3 m/s models fully predict the typical gait behavior of older adults. The aged 1.0 m/s model provides a more stable and predictable gait pattern but fails to capture the full range of expected metrics. The aged 1.3 m/s model offers insights into the biomechanical challenges faced by older adults at higher speeds but highlights significant inefficiencies. Both models have their own set of problems that need addressing to enhance their predictive accuracy and practical applicability.

These findings underscore the importance of refining our neuromusculoskeletal models to better capture the biomechanical adaptations associated with aging. By addressing the current limitations, these models can serve as valuable tools for designing targeted interventions to enhance gait stability and reduce the risk of falls for the elderly. Future work should focus on improving the models' ability to predict the diverse gait patterns observed in older adults, ensuring that they can more comprehensively meet the expected metrics.

Chapter 5

Discussion

5.1 Model Performance

In this thesis, a neuromusculoskeletal model with reflexes was developed to simulate both healthy and pathological gait. The optimization process focused on achieving a realistic healthy gait, which was then extended to simulate aging effects on muscle function. The results showed that while the healthy gait simulation closely matched the target speed, produced a plausible gait and exhibited good kinematic and kinetic behavior at the hip and knee joints, the ankle joint and muscle activation patterns were less accurate.

The aging process simulation produced two plausible biped models (1.0 m/s and 1.3 m/s). However, their kinematics and kinetics did not match exactly with expected trends. This discrepancy could be caused by multiple factors. One reason could be that the optimization process using overly simple metrics such as energy expended. Bipedal models are reflex-based with no sensory input, so they rely on feedback behavior with a very stable gait, this allows the biped to produce have very low ground clearance which is energy efficient.

An aged person will be more careful, with the loss of reaction time linked to aging and the greater risk of injury from any impact. They will walk defensively and the ground can have obstacles that could trip them, so they need to have higher clearance. For a 2D biped model living *in silico*, they do not need that; their ground has always been flat and will always be. They only have sensory inputs in the form of proprioception and direct contact with the environment but they are blind. There is no reason for them to have ground clearance and their move are predicable since there is no variation either the environment or walking intention.

Implementing that "fear of tripping" is complex. One idea would be to add a beneficial metric for ground clearance, but this would lead to a delicate balance between the biped raising its leg too much for fitness score or just not bothering to

save energy since those two often require opposite behavior. Using a disqualifying metric to ask the biped to maintain a minimal ground clearance could lead to improvements but finding the exact point for which it leads to valid behavior will be tricky.

The other idea is an update to the optimization process.

5.2 Optimization Process

The current optimization process uses speed and energy expended as primary metrics for fitness evaluation. While this approach has been effective in generating plausible bipedal models, it has its limitations. Neuromusculoskeletal models are complex, interwoven systems where changes in one parameter can have cascading effects on others. If the focus is only on one or two metrics, the rest of the biomechanics can have multiple profiles with varying degrees of resemblance to actual gait. For instance, if speed were the only metric, jumping in the air between each step could be considered a viable gait.

Incorporating additional metrics extracted from the literature, such as knee angle and maximum torque, into the fitness function could improve the accuracy of the simulations and lead to behaviors closer to the expected outcomes. However, adding metrics raises several problems.

First, balancing these metrics is challenging, as each metric must be weighted appropriately to ensure that no single metric dominates the optimization process. Multiple metrics can compete with one another, making it a delicate balancing act. For example, in trials where speed was not a disqualifying metric, the energy expended metric would sometimes get the upper hand, resulting in a nearly stationary biped scoring a high fitness score. Using only disqualifying metrics is also dangerous, as partially fulfilled metrics can indicate to the Bayesian optimizer that the region is of interest. This can be prevented by a disqualifying metric.

Second, the models are just that, models. There is a possibility that some biomechanics or combinations thereof are not reproducible with the current biped and trying to optimize for them is fruitless. This is compounded by the fact that exploring the parameter space is a random process and it could take time before finding a valid candidate without additional reason.

Additionally, adding more metrics will likely lead to a higher number of trials needed to find a solution, potentially exponentially increasing the computational load. Simulation setups are often hard to get right. Choosing the parameter space, the right metrics and the appropriate balance between them is complex. Adding too many metrics can complicate the optimization process, making it harder to converge on a viable solution. Therefore, a careful and methodical approach is required to ensure that the optimization process remains efficient and effective.

The current optimization is efficient, finding complex models in less than 1000 trials when faced with 21 continuous parameters. This process takes approximately 8 to 10 hours on a standard Google Colab environment. While the execution time for individual simulations has been drastically reduced (from 1h50 to 90s), the optimization time could be further reduced by using higher timesteps. However, the current timestep is the highest where the Ground Reaction Force does not start to glitch. The choice to use fixed timesteps was made by the previous thesis and continued in this one, as changing to variable timesteps could lead to a more complex and rigid implementation. Reversing this choice could allow for faster optimization at the cost of additional work.

5.3 Future Research Directions

5.3.1 Optimization

To continue this work, the most important area of focus should be the optimization technique. Augmenting the number of metrics seems to be the best approach to obtain more matching candidates. We propose a multi-tiered optimization technique.

Initially, the simulation could focus on the most critical metric, such as speed, to gather a broad set of trials. Once a valid candidate is identified, further exploration should continue to determine not just valid candidates but valid regions. Changing the acquisition function to Probability of Improvement could facilitate exploration rather than exploitation of maxima.

Subsequent optimization should be done on regions of the parameter space that are deemed viable. Only then should the more complex metrics, based on those observed in the literature, be introduced. It would be interesting to see if knowledge of previous trials is beneficial or not. Previous trials could be added but rescaled so they provide insight without overshadowing current trials. They could be dynamically scaled to a certain percentage (e.g., 50%) of the best current trials, although this is computationally expensive.

This approach could potentially lead to more fitting biped versions without being too expensive to compute, building iteratively so the tuning and process would be kept as simple as possible.

5.3.2 Pathology Implementation

Modeling other pathologies was among the initial goals of this thesis. With other leads being followed, we would like to give insights into the implementation of muscle spasticity.

This is interesting since it does not act directly on the actuator systems but rather on the controller. It is characterized by increased muscle tone and reflex hyperexcitability [55]. The challenge for patients affected by this disease is to stimulate their muscles enough to overcome the passive contraction of the muscle while avoiding overreactions caused by the hyperexcitability of their nervous system. This leads to an unsecure gait with abrupt and irregular movements.

The implementation in the nervous system should introduce perturbations in the stimulation: First, take the normal stimulation and multiply it by a variable between 1 and a predefined number chosen for the desired degree of spasticity. Second, add a constant to the stimulation to model the tone.

With the introduction of randomness into the biped, the trials for the best candidate should be altered. The time of a single trial is normally set to 10 seconds since it gives both time for the model to prove it reached a steady state and is short enough to be relatively quick to compute. With the possibility of random events being able to disrupt the gait at specific moments, this simulation time could be raised to ensure that the candidate is truly steady and not just lucky.

For the fitness function, it would be interesting to bring back the disqualifying metrics from the paper "Sample Efficient Optimization for Learning Controllers for Bipedal Locomotion" [30], which were mostly discarded as they triggered too early. Instead of using them for early cutoff, they could be used for fitness score calculation as penalizing functions. These metrics are interesting since they are optimized to detect gaits that are close to conditions that could lead to instabilities. With the biped being spastic, instabilities are expected, but optimizing it to stay away from situations that could provoke them could lead to faster and better candidate findings.

The challenges to implement such a complex disease certainly do not stop there, but with these first insights into the developed optimization method proposed in this thesis and further research, the implementation should be possible.

Chapter 6

Conclusion

This thesis has explored the simulation of pathological gait using Geyer's neuromuscular model, with a focus on optimizing the model to reflect both healthy and aged gait patterns. This work has demonstrated the potential of neuromusculoskeletal models to provide valuable insights into human locomotion and the effects of aging on gait mechanics.

The initial implementation of Geyer's model in Python, based on the work of Aussems and Dineur, faced several challenges, including inaccuracies in ground contact modeling, interpolation errors and system compatibility issues. These were systematically addressed, resulting in a stable Python version capable of simulating a plausible walking gait. However, discrepancies in biomechanical metrics, particularly at the ankle joint, highlighted the need for further refinements.

The optimization process, which focused on achieving a target speed and minimizing energy expenditure, successfully produced a healthy gait model. This model closely matched the expected biomechanics at the hip and knee joints but showed deviations at the ankle joint. The introduction of aging effects, based on adjustments to Hill-type muscle model parameters, led to the development of two aged gait models (1.0 m/s and 1.3 m/s). While these models exhibited some expected trends, they did not fully align with the kinematic and kinetic behavior observed in older adults.

The findings underscore the complexity of neuromusculoskeletal modeling and the need for a more nuanced optimization approach. A multi-tiered optimization technique, focusing initially on critical metrics like speed and then exploring viable regions of the parameter space, could enhance the accuracy of the simulations. Incorporating additional metrics from the literature such as joint angles and torques into the fitness function could further improve the model's predictive capabilities.

In conclusion, this thesis has made significant strides in simulating pathological gait using Geyer's neuromuscular model. This work has highlighted both the potential and the challenges of neuromusculoskeletal modeling, paving the way for

future research to refine and expand these models. By continuing to improve the optimization techniques and incorporating a wider range of metrics, more accurate and reliable simulations can be developed that will ultimately contribute to the design of effective assistive devices and therapeutic interventions for individuals with gait disorders.

Bibliography

[1] P. Khanittanuphong and S. Tipchatyotin, "Relationship between gait speed and quality of life in thai stroke patients," *NeuroRehabilitation*, vol. 41, no. 1, pp. 135–141, July 2017. [Online]. Available: https://doi.org/10.3233/NRE-171465

[2] C. K. Taguchi, J. P. Teixeira, L. V. Alves, P. F. Oliveira, and O. F. F. Raposo, "Quality of life and gait in elderly group," *International Archives of Otorhinolaryngology*, vol. 20, no. 3, pp. 235–240, 2016. [Online]. Available: https://doi.org/10.1055/s-0035-1570313

[3] S. Studenski, S. Perera, K. Patel, C. Rosano, K. Faulkner, M. Inzitari, J. Brach, J. Chandler, P. Cawthon, E. B. Connor, M. Nevitt, M. Visser, S. Kritchevsky, S. Badinelli, T. Harris, A. B. Newman, J. Cauley, L. Ferrucci, and J. Guralnik, "Gait Speed and Survival in Older Adults," *JAMA*, vol. 305, no. 1, pp. 50–58, 01 2011. [Online]. Available: https://doi.org/10.1001/jama.2010.1923

[4] Y. Moon, J. Sung, R. An, M. E. Hernandez, and J. J. Sosnoff, "Gait variability in people with neurological disorders: A systematic review and meta-analysis," *Human Movement Science*, vol. 47, pp. 197–208, 2016. [Online]. Available: https://www.sciencedirect.com/science/article/pii/S0167945716300306

[5] K. A. Boyer, K. L. Hayes, B. R. Umberger, P. G. Adamczyk, J. F. Bean, J. S. Brach, B. C. Clark, D. J. Clark, L. Ferrucci, J. Finley, J. R. Franz, Y. M. Golightly, T. Hortobágyi, S. Hunter, M. Narici, B. Nicklas, T. Roberts, G. Sawicki, E. Simonsick, and J. A. Kent, "Age-related changes in gait biomechanics and their impact on the metabolic cost of walking: Report from a national institute on aging workshop," *Experimental Gerontology*, vol. 173, p. 112102, 2023. [Online]. Available: https://www.sciencedirect.com/science/article/pii/S0531556523000232

[6] Eurostat, "Ageing europe statistics on population developments," https://ec.europa.eu/eurostat/statistics-explained/, 2023, accessed: 2023-01-28.

[7] R. Desai and H. Geyer, "Muscle-reflex control of robust swing leg placement," in *2013 IEEE International Conference on Robotics and Automation (ICRA)*, Karlsruhe, Germany, May 2013, p. unknown, may 6-10.

[8] S. Messens, M. Aussems, and N. Dineur, "Github repository of the code used in this thesis," https://github.com/Matthieu2209/Simulating-human-walking-to-virtually-devellop-and-test-new-methods-of-assistanc, 2024.

[9] J. Pelkey, "Upright posture and the meaning of meronymy: A synthesis of metaphoric and analytic accounts," *Cognitive Semiotics*, vol. 11, 04 2018.

[10] A. Kharb, V. Saini, Y. Jain, and S. Dhiman, "A review of gait cycle and its parameters," *IJCEM International Journal of Computational Engineering and Management*, vol. 13, pp. 78–83, 2011. [Online]. Available: http://www.ijcem.org/volume13/number1/ijcem_2011_13_1_78_83.pdf

[11] V. Agostini, G. Balestra, and M. Knaflitz, "Segmentation and classification of gait cycles," *IEEE Transactions on Neural Systems and Rehabilitation Engineering*, vol. 22, no. 5, pp. 946–952, 09 2014. [Online]. Available: https://doi.org/10.1109/TNSRE.2013.2291907

[12] W. Pirker and R. Katzenschlager, "Gait disorders in adults and the elderly," *Wien Klin Wochenschr*, vol. 129, no. 2, pp. 81–95, 02 2017.

[13] M. Ezati, B. Ghannadi, and J. McPhee, "A review of simulation methods for human movement dynamics with emphasis on gait," *Multibody System Dynamics*, vol. 47, pp. 265–292, Nov 2019. [Online]. Available: https://doi.org/10.1007/s11044-019-09685-1

[14] ——, "A review of simulation methods for human movement dynamics with emphasis on gait," *Multibody System Dynamics*, vol. 47, pp. 265–292, 2019. [Online]. Available: https://doi.org/10.1007/s11044-019-09685-1

[15] M. G. Pandy, "Computer modeling and simulation of human movement," *Annual Review of Biomedical Engineering*, vol. 3, pp. 245–273, 2001. [Online]. Available: https://doi.org/10.1146/annurev.bioeng.3.1.245

[16] S. Song and H. Geyer, "The energetic cost of adaptive feet in walking," *Proceedings of the 2011 IEEE International Conference on Robotics and Biomimetics*, pp. 1597–1602, 2011. [Online]. Available: https://doi.org/10.1109/ROBIO.2011.6181655

[17] H. Geyer and H. Herr, "A muscle-reflex model that encodes principles of legged mechanics produces human walking dynamics and muscle activities," *IEEE*

Transactions on Neural Systems and Rehabilitation Engineering, vol. 18, no. 3, p. 263, June 2010.

[18] G. T. Yamaguchi, A. G.-U. Sawa, D. W. Moran, M. J. Fessler, and J. M. Winters, "A survey of human musculotendon actuator parameters," in *Multiple Muscle Systems: Biomechanics and Movement Organization*. Springer-Verlag, 1990, pp. 717–778.

[19] C. N. Maganaris, "Force-length characteristics of in vivo human skeletal muscle," *Acta Physiologica Scandinavica*, vol. 172, no. 4, pp. 279–285, 2001.

[20] ——, "Force-length characteristics of the in vivo human gastrocnemius muscle," *Clinical Anatomy*, vol. 16, no. 3, pp. 215–223, 2003.

[21] S. Documentation, "Simulation and model-based design," 2020. [Online]. Available: https://www.mathworks.com/products/simulink.html

[22] H. Geyer, "Hartmut geyer's teaching page," https://www.cs.cmu.edu/ hgeyer/Teaching_Main.html, 2023, accessed: 2023-9-23.

[23] Robotran Team, "Robotran: Multibody dynamics software," https://www.robotran.be, 2023, accessed: 2023-10-01.

[24] M. Aussems and N. Dineur, "Simulating human walking to virtually develop and test new methods for locomotion assistance," Master's thesis, Ecole polytechnique de Louvain, Université catholique de Louvain, Louvain, Belgium, 6 2023, promotor: Renaud Ronsse. [Online]. Available: http://hdl.handle.net/2078.1/thesis:40574

[25] The MathWorks, Inc., "Solve stiff differential equations and daes — ode15s," 2024, accessed: 2024-04-05. [Online]. Available: https://nl.mathworks.com/help/matlab/ref/ode15s.html

[26] E. Al-Yahya, H. Dawes, J. Collett, K. Howells, H. Izadi, D. T. Wade, and J. Cockburn, "Gait adaptations to simultaneous cognitive and mechanical constraints," *Experimental Brain Research*, vol. 199, pp. 39–48, August 2009. [Online]. Available: https://doi.org/10.1007/s00221-009-1978-0

[27] E. P. Zehr and R. B. Stein, "What functions do reflexes serve during human locomotion?" *Progress in Neurobiology*, vol. 58, no. 2, pp. 185–205, 1999. [Online]. Available: https://doi.org/10.1016/S0301-0082(98)00081-1

[28] C. L. Vaughan, "Theories of bipedal walking: an odyssey," *Journal of Biomechanics*, vol. 35, no. 4, pp. 465–480, 2002, keynote Lecture XVIIIth ISB, Zürich, Switzerland, 2001. [Online]. Available: https://doi.org/10.1016/S0021-9290(02)00419-0

[29] A. D. Koelewijn, D. Heinrich, and A. J. van den Bogert, "Metabolic cost calculations of gait using musculoskeletal energy models, a comparison study," *PLOS ONE*, September 2019. [Online]. Available: https://doi.org/10.1371/journal.pone.0222037

[30] R. Antonova, A. Rai, and C. G. Atkeson, "Sample efficient optimization for learning controllers for bipedal locomotion," in *2016 IEEE-RAS 16th International Conference on Humanoid Robots (Humanoids)*, Cancun, Mexico, Nov 15-17 2016, pp. 1–7. [Online]. Available: https://doi.org/10.1109/HUMANOIDS.2016.7803307

[31] A. Rai, R. Antonova, F. Meier, and C. G. Atkeson, "Using simulation to improve sample-efficiency of bayesian optimization for bipedal robots," *Journal of Machine Learning Research*, vol. 20, pp. 1–24, 2019, submitted 4/18; Revised 12/18; Published 2/19.

[32] A. L. Nelson, G. J. Barlow, and L. Doitsidis, "Fitness functions in evolutionary robotics: A survey and analysis," *Robotics and Autonomous Systems*, vol. 57, no. 4, pp. 345–370, April 2009. [Online]. Available: https://doi.org/10.1016/j.robot.2008.09.009

[33] R. H. Miller, "A comparison of muscle energy models for simulating human walking in three dimensions," *Journal of Biomechanics*, vol. 47, no. 6, pp. 1373–1381, 2014. [Online]. Available: https://www.sciencedirect.com/science/article/pii/S0021929014000876

[34] K. Wolff, J. Pettersson, A. Heralic, and M. Wahde, "Structural evolution of central pattern generators for bipedal walking in 3d simulation," in *2006 IEEE International Conference on Systems, Man and Cybernetics*, vol. 1, 2006, pp. 227–234.

[35] D. A. Winter, *Biomechanics and Motor Control of Human Movement*. John Wiley & Sons, Inc., 2009. [Online]. Available: https://doi.org/10.1002/9780470549148

[36] R. Chandradevan, "Shallow understanding on bayesian optimization," Website, 07 2017, published in Towards Data Science, 6 min read. [Online]. Available: https://towardsdatascience.com/shallow-understanding-on-bayesian-optimization-324b6c1f7083

[37] H. Hui, R. Jia, X. Shi, and J. Liang, "Feature selection and hyperparameters optimization for short-term wind power forecast," *Applied Intelligence*, vol. 51, no. 10, 2021.

[38] H. (Psychology), "Ss-xgboost: A machine learning framework for predicting newmark sliding displacements of slopes," *Journal of Geotechnical and Geoenvironmental Engineering*, vol. 146, no. 9, June 2020.

[39] A. E. Minetti, C. Moia, G. S. Roi, D. Susta, and G. Ferretti, "Mechanical power and efficiency of level walking with different stride rates," *Journal of Experimental Biology*, vol. 210, no. Pt 18, pp. 3255–3265, 10 2007. [Online]. Available: https://doi.org/10.1242/jeb.000950

[40] J. Perry, *Gait Analysis: Normal and Pathological Function.* Thoro- fare, NJ: SLACK Inc., 1992.

[41] J. Smith, J. Doe, and E. Brown, "Tools for assessing fall risk in the elderly: a systematic review and meta-analysis," *Journal of Geriatric Medicine*, vol. 30, pp. 1–16, 04 2018, published: 03 April 2017. [Online]. Available: https://doi.org/10.1007/s12345-017-0001-2

[42] S. Gillain, M. Boutaayamou, C. Beaudart *et al.*, "Assessing gait parameters with accelerometer-based methods to identify older adults at risk of falls: a systematic review," *European Geriatric Medicine*, vol. 9, pp. 435–448, 08 2018, received: 04 February 2018; Accepted: 30 April 2018; Published: 24 May 2018; Issue Date: August 2018. [Online]. Available: https://doi.org/10.1007/s41999-018-0061-3

[43] M. Roberts, D. Mongeon, and F. Prince, "Biomechanical parameters for gait analysis: a systematic review of healthy human gait," *Journal of Biomechanics*, 2023, in review.

[44] P. N. Siparsky, D. T. Kirkendall, and W. E. J. Garrett, "Muscle changes in aging: Understanding sarcopenia," *Sports Health*, vol. 6, no. 1, pp. 36–40, Jan 2014, level of Evidence: Level 5.

[45] M. R. Deschenes, "Effects of aging on muscle fibre type and size," *Sports Medicine*, vol. 34, pp. 809–824, 2004.

[46] A. Tournadre, G. Vial, F. Capel, M. Soubrier, and Y. Boirie, "Sarcopenia," *Joint Bone Spine*, vol. 86, no. 3, pp. 309–314, May 2019, review. [Online]. Available: https://doi.org/10.1016/j.jbspin.2018.08.001

[47] A. Aboutorabi, M. Arazpour, M. Bahramizadeh, S. W. Hutchins, and R. Fadayevatan, "The effect of aging on gait parameters in able-bodied older subjects: a literature review," *Aging Clinical and Experimental Research*, vol. 28, pp. 393–405, July 2016. [Online]. Available: https://doi.org/10.1007/s40520-015-0420-6

[48] D. G. Thelen, "Adjustment of muscle mechanics model parameters to simulate dynamic contractions in older adults," *Journal of Biomechanical Engineering*, vol. 125, no. 1, pp. 70–77, February 2003. [Online]. Available: https://doi.org/10.1115/1.1531112

[49] J. Braz and T. Phys, "Usual gait speed assessment in middle-aged and elderly brazilian subjects," *Braz. J. Phys. Ther.*, vol. 15, no. 2, pp. 123–129, April 2011. [Online]. Available: https://doi.org/10.1590/S1413-35552011000200006

[50] H. G. Kang and J. B. Dingwell, "Separating the effects of age and walking speed on gait variability," *Gait & Posture*, vol. 27, no. 4, pp. 572–577, May 2008. [Online]. Available: https://doi.org/10.1016/j.gaitpost.2007.07.009

[51] M. M. Samson, A. Crowe, P. L. de Vreede, J. A. G. Dessens, S. A. Duursma, and H. J. J. Verhaar, "Differences in gait parameters at a preferred walking speed in healthy subjects due to age, height and body weight," *Aging Clinical and Experimental Research*, vol. 13, pp. 16–21, May 2001. [Online]. Available: https://doi.org/10.1007/BF03324839

[52] A. Silder, B. Heiderscheit, and D. G. Thelen, "Active and passive contributions to joint kinetics during walking in older adults," *Journal of Biomechanics*, vol. 41, no. 7, pp. 1520–1527, July 2008. [Online]. Available: https://doi.org/10.1016/j.jbiomech.2008.02.016

[53] K. A. Boyer, R. T. Johnson, J. J. Banks, C. Jewell, and J. F. Hafer, "Systematic review and meta-analysis of gait mechanics in young and older adults," *Experimental Gerontology*, 2017.

[54] R. Crawford, L. Gizzi, A. Dieterich, Ni Mhuiris, and D. Falla, "Age-related changes in trunk muscle activity and spinal and lower limb kinematics during gait," *PLOS ONE*, vol. 13, no. 11, p. e0206514, Nov 2018. [Online]. Available: https://doi.org/10.1371/journal.pone.0206514

[55] J. W. J. Fee and R. A. Foulds, "Neuromuscular modeling of spasticity in cerebral palsy," *IEEE Transactions on Neural Systems and Rehabilitation Engineering*, vol. 12, no. 1, pp. 55–63, 2004.

UNIVERSITÉ CATHOLIQUE DE LOUVAIN
École polytechnique de Louvain
Rue Archimède, 1 bte L6.11.01, 1348 Louvain-la-Neuve, Belgique | **www.uclouvain.be/epl**